



# HHS Public Access

Author manuscript

*J Med Chem.* Author manuscript; available in PMC 2023 September 09.

Published in final edited form as:

*J Med Chem.* 2023 March 09; 66(5): 3372–3392. doi:10.1021/acs.jmedchem.2c01858.

## Metabolism-Guided Selective Androgen Receptor Antagonists: Design, Synthesis, and Biological Evaluation for Activity against Enzalutamide-Resistant Prostate Cancer

**Dong-Jin Hwang,**

Department of Pharmaceutical Sciences, University of Tennessee Health Science Center, Memphis, Tennessee 38163, United States

**Yali He,**

Department of Pharmaceutical Sciences, University of Tennessee Health Science Center, Memphis, Tennessee 38163, United States

**Suriyan Ponnusamy,**

Department of Medicine, University of Tennessee Health Science Center, Memphis, Tennessee 38163, United States

**Thirumagal Thiyagarajan,**

Department of Medicine, University of Tennessee Health Science Center, Memphis, Tennessee 38163, United States

**Michael L. Mohler,**

Department of Pharmaceutical Sciences, University of Tennessee Health Science Center, Memphis, Tennessee 38163, United States

**Ramesh Narayanan,**

Department of Medicine, University of Tennessee Health Science Center, Memphis, Tennessee 38163, United States

**Duane D. Miller**

Department of Pharmaceutical Sciences, University of Tennessee Health Science Center, Memphis, Tennessee 38163, United States

### Abstract

---

**Corresponding Author: Duane D. Miller** – Department of Pharmaceutical Sciences, University of Tennessee Health Science Center, Memphis, Tennessee 38163, United States; Phone: +1-901-448-6026; dmiller@uthsc.edu; Fax: +1-901-448-3446.

Author Contributions

The manuscript was written through contributions of all authors. All authors have given approval to the definitive version of the manuscript.

The authors declare no competing financial interest.

Complete contact information is available at: <https://pubs.acs.org/10.1021/acs.jmedchem.2c01858>

Supporting Information

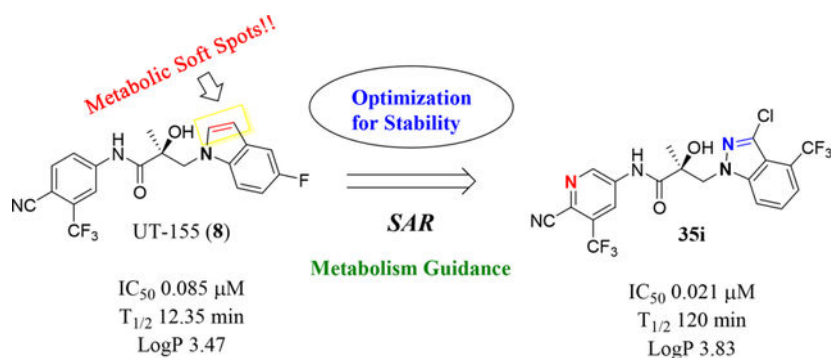
The Supporting Information is available free of charge at <https://pubs.acs.org/doi/10.1021/acs.jmedchem.2c01858>.

Molecular formula strings (CSV)

Additional information on compound characterization, additional biological experiments, and figures (PDF)

A major challenge for new drug discovery in the area of androgen receptor (AR) antagonists lies in predicting the druggable properties that will enable small molecules to retain their potency and stability during further studies *in vitro* and *in vivo*. Indole (compound **8**) is a first-in-class AR antagonist with very high potency ( $IC_{50} = 0.085 \mu M$ ) but is metabolically unstable. During the metabolic studies described herein, we synthesized new small molecules that exhibit significantly improved stability while retaining potent antagonistic activity for an AR. This structure–activity relationship (SAR) study of more than 50 compounds classified with three classes (Class I, II, and III) and discovered two compounds (**32c** and **35i**) that are potent AR antagonists (e.g.,  $IC_{50} = 0.021 \mu M$ ,  $T_{1/2} = 120$  min for compound **35i**). The new antagonists exhibited improved *in vivo* pharmacokinetics (PK) with high efficacy antiandrogen activity in Hershberger and antiandrogen Enz-Res tumor xenograft models that overexpress AR (LNCaP-AR).

### Graphical Abstract:



## 1. INTRODUCTION

Human androgen receptors (ARs) and the development of antiandrogenic ligands are principal drivers for diseases characterized by AR abnormality, including prostate cancer (PC).<sup>1</sup> The number of PC patients in the United States and worldwide continues to increase.<sup>2</sup> As a key molecule in the progression of PC, AR is a critical therapeutic target for developments of treatments for castration-resistant PC (CRPC).<sup>3</sup> Despite the FDA approval of antiandrogens for treatment of PC, the emergence of antiandrogen-resistant forms of PC remains a challenge to this therapeutic scheme that will require innovative approaches to solve.

AR is a steroid receptor transcription factor that is activated by androgenic hormones such as testosterone (T) and  $5\alpha$ -dihydrotestosterone (DHT). The three main functional AR domains are the N-terminal domain that contains activation function-1 (AF-1), the DNA-binding domain that binds to the promoters and enhancers that regulate AR-dependent genes and contains the hinge region, and the ligand-binding domain (LBD) that contains AF-2 and binds to endogenous androgens.<sup>4</sup> Androgen deprivation therapy (ADT) blocks the endogenous testicular production of androgens and effectively lowers serum T to castration levels. ADT has been the standard of care for advanced PC and has been used for combination therapy with antiandrogens (direct AR antagonists) such as bicalutamide, enzalutamide, apalutamide, darolutamide, and abiraterone acetate,<sup>5–10</sup> as shown in Figure

1. Thus far, antiandrogens have typically been diaryl compounds with two aromatic rings connected by a propanamide segment (Figure 1, compounds **1–4**) that can be linear (Figure 1, compounds **1,4**) or cyclized into a hydantoin (Figure 1, compounds **2–3**). When members of our group modified the B-ring, we discovered a class of nonsteroidal tissue-selective androgen receptor modulators (SARMs)<sup>11–20</sup> that function as tissue-selective agonists (Figure 1, compounds **6–7**). In contrast, inclusion of a basic nitrogen atom to replace the thioether or ether group in the SARM compounds resulted in a new class of compounds that exhibit pan-antagonism and selective androgen receptor degrader (SARD) activity (Figure 1, compounds **8–9**).<sup>13,21–24</sup>

The first-in-class AR antagonist UT-155 (Figure 1, compound **8**), unlike enzalutamide (Figure 1, compound **2**), contained an indolyl group in place of the B-ring and exhibits exceptionally potent AR degrader activity ( $IC_{50} = 0.085 \mu M$  for UT-155 and  $216 \mu M$  for enzalutamide).<sup>13,21</sup>

The discovery that **UT-155** also contained a site that was metabolically labile ( $T_{1/2} = 12.34$  min) in human liver microsomes (HLM) led us to investigate the 2- and 3-positions of the indole B-ring in an effort to develop compounds with improved antimitotic effects and reduced untoward effects such as metabolic instability. Generally, strategies for reducing the metabolism of a drug include reducing lipophilicity, modulating steric and electronic factors, altering stereochemistry, and introducing conformational constraints during the drug discovery process.<sup>25</sup> However, the knowledge from our initial biological evaluation of the B-rings from the different indole types (Table 1) suggested that since the 2- and 3-positions on the indole ring were possible metabolic weak spots, they might be most amenable to modification.

In comparing metabolic stability of the 2,3-unsubstituted indole **8** ( $T_{1/2} = 12.35$  min showed in Table 1) with substituted 3-position groups, effects on the 3-position introducing electron withdrawing group (EWG, e.g., compound **19a**;  $T_{1/2} = 21.77$  min in Table 1) or electron donating group (EDG, e.g., compound **19b**;  $T_{1/2} = 9.29$  min) showed different stability in the mouse model by possibly blocking the metabolism shown in Figure 3. It was observed in our initial test in Table 1 that the EWGs and EDGs on the 3-position of the indole core can change the stability trend for our indole derivatives.

Indoles are one of the main functional groups found in natural and synthesized drugs, as shown in Figure 2. After our structural analysis of known indoles, we categorized them into four types (A, B, C, and D) based on the substitutions added to the 2- and/or 3-positions of the core indole portion. Indole groups of Type A are unsubstituted, i.e., have no substituents at the 1-, 2-, or 3-positions of the indole ring (depicted by the NH group at position 1, Figure 2A) and are typified by pindolol<sup>26</sup> (Figure 2, compound **10**), an antihypertensive drug that functions as an antidepressant. Indoles of Type B have a substituent only at the 2-position of the core indole (Figure 2B). These include betanin<sup>27</sup> (Figure 2B, compound **11**), which lowers blood pressure, and delaviridine<sup>28</sup> (Figure 2B, compound **12**), a non-nucleoside reverse transcriptase inhibitor (NNRTI) of human immunodeficiency virus (HIV). Indoles of Type C have a substituent only at the 3-position of the core indole (Figure 2C). These are typified by the antihypertensive drug oglufanide disodium<sup>29</sup> (Figure 2C, compound **13**),

the neurotransmitter serotonin<sup>29</sup> (Figure 2C, compound **14**), and the antidepressant drug tryptophan<sup>29,30</sup> (Figure 2C, compound **15**). Finally, indoles of Type D are disubstituted at both the 2- and 3-positions of the core indole (Figure 2D). These are typified by the anti-inflammatory drug indomethacin<sup>4</sup> (Figure 2D, compound **16**), the sexual dysfunction drug yohimbine<sup>31</sup> (Figure 2D, compound **17**), and the broad-spectrum antiviral drug Arbidol<sup>32</sup> (Figure 2D, compound **18**).

The mechanism for the *in vivo* and *in vitro* metabolism of indole groups proposed by Claus et al. (1983), shown schematically in Figure 3, features oxidation of the indole ring at the 3-position to yield an indoxyl group, followed by either glycosylation at the 3-position, which targets the molecule for degradation, or oxidation at 2-position to yield an isatin group that is subject to oxidative cleavage of the five-membered pyrrole constituent of the heterobicyclic ring; additional oxidation results in the cleavage of the indole ring.<sup>33,34</sup> Herein, we report a metabolism-guided approach that optimized substituents in the 2- and 3-positions on the indole group in the B-ring of UT-155 (Figure 1, compound **8**) to yield metabolically stable indole analogues that exhibit significant AR antagonist activity. In this study, we sought to produce new molecules that will potently inhibit AR with binding stronger than 0.200  $\mu\text{M}$  and high metabolic stability (i.e., longer half-life ( $T_{1/2}$ ) than that of UT-155 (12.35 min) and optimally >60 min).

## Chemistry.

**Design Strategy and Initial Test.**—We performed a structure–activity relationship (SAR) study, shown schematically in Figure 4, with which to explore potential metabolic sites at the 2- and 3-positions of the indole ring, using as our starting point the indole of UT-155 (Figure 1, compound **8**) developed from the amine UT-69 (Figure 1, compound **9**).<sup>13</sup> To further optimize UT-155 (compound **8**) and lengthen its short metabolic half-life, we first protected the 2- and 3-positions of its indole portion with different blocking modes using the following Class I–III changes:

- Class I: bulky/hard modes with 2- and 3-positioned indoles (called as carbazole (compounds in series **27**) and benzotriazole derivatives (compounds in series **34**)).
- Class II: 2- or 3-positioned indoles that are derivatives of benzimidazole (called “3N-indole”, compounds in series **31**) and indazole (called as “2N-indole”, compounds in series **32**).
- Class III: 3-substituted 2N-indoles (called “3-substituted indazoles”) that led to substituted indazole compounds (series **35**).

Using this strategy (Figure 4), we designed and synthesized more than 50 new chiral AR indoles using the three different blocking methods (Class I, II, and III); their structures are summarized in Table 2. We subsequently assayed their metabolic stability and potency.

## RESULTS AND DISCUSSION

### 2.1. Chemistry.

We will begin by describing the preparation of newly designed molecules of Classes I, II, and III. Using methods described in the literature,<sup>11,13</sup> we coupled the bromide compound **23** with various substituted heterocyclic compounds (carbazoles, benzimidazoles, substituted indoles, benzotriazoles, or indazoles; i.e., compounds **25**, **28**, **29**, or **30**) in the presence of various bases to produce compounds **27**, **31**, **32**, **34**, and **35**, as shown in Schemes 1, 2, and 3. Notably, for Class I, sodium hydride (NaH) was effectively used to activate carbazoles in compound **25** and reacted with related bromides in compound **23** to produce good yields (>80%) of the targeted carbazole molecules **27a–e**, following the preparation of the bromoacid compound **22** and the subsequent aniline compound **21** in the procedure we described previously,<sup>11,13</sup> as shown in Scheme 1.

For Class II, compounds **31a–g** were prepared using three different bases, namely NaH in THF (Method A), K<sub>2</sub>CO<sub>3</sub> in DMF (Method B), or bis(trimethylsilyl)amide in THF (Method C), as shown in Scheme 2. Benzimidazole derivatives of compounds **31a–b** were prepared by NaH-mediated activation in general Method A (see Experimental Section) and purified with their regiospecific isomers by flash column chromatography, followed by confirmation of the presence of both regiospecific isomers (1*N*-alkylated benzimidazole B-ring for compound **31a** and 2*C*-alkylated benzimidazole B-ring for compound **31b**). A measurement of *N*- and *C*-alkylation yielded a 1:2 ratio (i.e., 12.6% for compound **31a**: 28.4% for compound **31b**, with a total yield of 41% via Scheme 2).

1*N*-Alkylation of compound **31c** was predominantly produced using potassium carbonate (K<sub>2</sub>CO<sub>3</sub>) in DMF at 80 °C (Method B) to couple the bromide compound **23c** with 4-fluorobenzimidazole (compound **29** with R<sub>1</sub> = F, Scheme 2) with 63% yield. Pairs of regioisomers (compounds **31d–e** and **31f–g**) were obtained by treating the corresponding benzimidazole compound **29** with lithium bis(trimethylsilyl)amide and bromide compounds **23a–c** followed by separation using column chromatography. Using NaH in THF solution,<sup>13,35</sup> the 3-substituted indole compound **28** underwent *N*-alkylation with compound **23** (**23a** or **23b**) to produce the desired indolyl compounds **31h–s** in reasonable yields (<94%) via Scheme 2. The addition of nucleophilic hydroxylamine (or acetohydrazide) to aldehyde compounds **31i** or **31m** in basic conditions produced the designed compounds **31n–p** by Method D (see Experimental Section). For indazole compounds **32a–d**, the reaction was conducted using bases (i.e., lithium bis(trimethylsilyl)amide for compounds **32a–b** or NaH for compounds **32c–d**), through *N*-substitution (i.e., 1*N*- and 2*N*- of an indazole) of indazole compound **30** with bromide compound **23** generated the pairs of regiospecific isomers (1*N*- and 2*N*-indazole compounds **32a–b** and **32c–d**, respectively, which were subsequently isolated by flash column chromatography. 2D NMR was used to identify the isomer pairs of benzimidazoles (compounds **31a–b** and **31f–g**) and indazoles (compounds **32a–b** and **32c–d**), as shown in Figure S1 and S2 of the Supporting Information section. The structures of the regiospecific isomers of the benzimidazoles (compounds **31a–b** and **31f–g**) and indazoles (compounds **32a–d**) are summarized in Table 3.

In Scheme 3, several benzo-triazole/3-substituted indazole derivatives (compounds **34a–g** and **35a–j**, Class I and III) were prepared by Method A, as reported previously.<sup>13</sup> A Suzuki reaction that entailed carbon–carbon cross-coupling<sup>36</sup> of a palladium(0) complex reaction of compound **34g** with phenyl boric acid produced the corresponding compound **34h** in good yield (90%). For the 3-substituted indazole compound **35** series, activation of several 3-substituted indazole compounds of **33** with sodium hydride produced the desired 3-substituted indazoles **35a–j** by Method A, as shown in Scheme 3.

## 2.2. Separation, Determination and Two Sets of Isomers (Benzimidazoles and Indazoles) in the B-Ring (Class II).

We successfully prepared three sets of regioisomeric isomers (compounds **31a–b**, **31d–e**, and **32a–d**) by synthetic Methods A or C and purified the sets of the isomers by flash column chromatography to produce each isomer of the benzimidazoles (isomers **31a–31b** and **31d–31e**) and the indazoles (isomers **32a–32b** and **32c–32d**).

The regioisomers of 1N- or 2C-benzimidazoles (compounds **31a–31b**), 1N- or 3N-benzimidazoles (compounds **31d** and **31e**; **31f** and **31g**), and 1N- or 2N-indazoles derivatives (**32a** and **32c**; **32b** and **32d**) were purified with flash column chromatography to produce each pair of isomers shown in Table 3 and Scheme 2. LC mass spectroscopy and 2D NMR were used to identify the separated sets of each isomer (**31a–b**, **31d–e**, and **32a–d**), as shown in Figures S1 and S2. Each B-ring isomer substituted with benzimidazole or indazole exhibited different retention times in HRMS analysis (Figure S1, panel **B** for **31f** and **31g** and Figure S1, panels **D** and **F** for compounds **32a–32d**), while 2D NMR identified the individual chemical structures by their different NOE effects (Figure S2, panels **A–F**). In our effort to further investigate the B-ring analogues including the benzimidazoles and indazoles produced by SAR (Figure 4), we next examined their bioactivity *in vitro*.

## 2.3. Overview of *in Vitro* Antagonism of AR Biological Activity (Class I–III Derivatives).

We first examined the effect of the B-ring substitutions (in Class I–III) on their ability to antagonize transcription of a luciferase reporter gene under control of a glucocorticoid response element (GRE-LUC) in the presence of AR agonist R1881 (IC<sub>50</sub>) in African green monkey COS cells.

The pharmacological activities of Class I, II, and III derivatives were examined *in vitro* using not only the transactivation assay for AR antagonism described here but also assays of AR binding affinity and degradation, as described in the legend of Table 4 (for Class I) and Table 5 (for Class II and III). The degradation assays were performed in two cell lines, the androgen-sensitive human prostate adenocarcinoma cell line LNCaP that expresses full-length (FL) AR and the xenograft-derived human prostate carcinoma epithelial cell line 22RV1 that expresses a c-terminally truncated splice variant (SV) of AR (AR-V7). The results obtained from AR affinity binding, AR antagonism, and AR degradation assays performed with Class I derivatives (indoles substituted at the 2- and 3-positions, compounds **27a–e** and **34a–h**) are shown in Table 4. The bulky carbazoles, compounds **27a–e**, exhibited consistent AR binding affinity (>0.810  $\mu\text{M}$  for compound **27e**) and degradation of FL AR in LNCaP cells (<51% at 1  $\mu\text{M}$  for compound **27e**) and in 22RV1 cells (<87% at 10  $\mu\text{M}$



for compound **27a**), as shown in Table 4. The AR transactivation ( $IC_{50}$ ) of compound **27b** ( $0.871 \mu M$ ) was not enhanced relative to parental indole compound **8** ( $0.085 \mu M$ ) or enzalutamide (compound **2**;  $0.216 \mu M$ ). For the triazole derivatives **34a–h**, in the AR transactivation assay of antagonistic activity ( $IC_{50}$ ), the 2N-substituted triazole (compound **34a**) exhibited similar transactivation ( $0.277 \mu M$ ) to that of enzalutamide (compound **2**;  $0.216 \mu M$ ). Finally, in the AR degradation assay, the triazole derivatives like compound **34a** degraded FL AR in LNCaP cells (70% for **34a**), but compounds **34a** and **34b** were unable to degrade the AR-7 AV mutant in 22RV1 cells (Table 4).

We next tested the effects of modifying the indole B-ring 2- or 3-positions (2N- or 3N-) in the Class II-blocked compounds **31a–s** and **32a–d** or both the 2- and 3-positions (2N- and 3N-) in the Class III-blocked compounds **35a–l** in the *in vitro* assays for binding affinity to the AR LBD ( $K_i$ ), antagonism of the wildtype (wtAR), and ability to degrade FL and SV AR (% degradation), as shown in Table 5. Of the Class II derivatives with benzimidazoles at the 3-position, compounds **31h–i** (3-F and 3-Cl benzimidazoles, respectively) exhibited strong AR binding affinity ( $K_i = 0.318 \mu M$  for compound **31h** and  $0.755 \mu M$  for compound **31i**) and reasonable transactivation of AR ( $IC_{50} = 0.274$  and  $0.367 \mu M$ , respectively).

The regiospecific isomers **31f** and **31g** (3N-substituted, Table 3) exhibited similar binding affinity for AR and similar levels of degradation of FL AR (50% and 64%, respectively), but neither degraded the AR SV mutant (Table 5). While compound **31g** retained the weak antagonistic activity for AR transactivation ( $IC_{50} = 3.616 \mu M$ ) like that observed for the 1N-substituted, compound **31f** exhibited no ability to inhibit this activity ( $IC_{50} > 100 \mu M$ ; Table 5). Compound **31j** (pyrido A-ring in compound **8**) exhibited very robust transactivation of AR- transactivation ( $IC_{50} = 0.021 \mu M$ ; Table 5), which is four times more active than compound **8** ( $0.085 \mu M$ ) and ten times more active than compound **2** ( $0.216 \mu M$ ). However, compound **31j** bound to AR less well ( $K_i = 0.757 \mu M$ ) than UT-155 (compound **8**;  $K_i = 0.267 \mu M$ ) but better than enzalutamide (compound **2**;  $K_i = 3.641 \mu M$ ), as shown in Table 5. Compounds **31m–q** with bulky groups at the 3-position exhibited low binding affinities for AR but strong inhibition of AR transactivation ( $IC_{50} = 0.746–0.134 \mu M$ ) by all of these compounds except for compound **31p** ( $IC_{50} = 3.434 \mu M$ ), as shown in Table 5. Interestingly, the presence of a nitro or cyano group on the 3N-indole in compounds **31r** and **31s** maintained or improved AR binding ( $K_i$ ) and suppression of AR transactivation activity ( $IC_{50}$ ) but did not improve stability (data not shown) compared with compound **8**.

When the 1N- or 2N-indazole compounds **32a–b** and **32c–d** (structures in Table 3), respectively (Table 5) were assessed for AR binding, antagonistic activity, and degradation (data not shown), the 1N-indazole compounds **32a** and **32c** were both able to degrade full length AR (92% and 84%, respectively, compared to compound **8**, 65–83%) but compound **32c** was better able to degrade the AR SV than compound **32a** or compound **8** (**32a**, 34%; **32c**, 100%; **8**, 60–100%). While compound **32a** exhibited weak antagonism of AR transactivation ( $IC_{50} = 0.173 \mu M$ ) and bound to AR better than control compound **8** ( $K_i = 0.267 \mu M$ ), compound **32c** exhibited poor AR transactivation inhibition ( $IC_{50} = 0.373 \mu M$ ) and AR binding ( $K_i = 1.006 \mu M$ ), as shown in Table 5. In contrast, neither of the 2N-indazole compounds **32b** and **32d** were able to degrade AR FL or SV (0%).

For the Class III, 3-substituted indazoles (compounds **35a-k**), compounds with an electron donating group in position 3 (e.g.,  $-\text{CH}_3$ , compound **35g**) exhibited extraordinarily strong antagonism for AR transactivation ( $\text{IC}_{50} = 0.0891 \mu\text{M}$  vs  $0.085 \mu\text{M}$  for compound **8**), as shown in Table 5. Other compounds with electron withdrawing groups (e.g., F, Cl, Br, and  $\text{CF}_3$  in compounds **35a-f**) exhibited stronger AR binding ( $0.102 \mu\text{M}$  for compound **35a**) and low-to-moderate degradation of FL AR (37% for compound **35a**), as shown in Table 5. The derivatives with nitrogen A-ring moieties (**35b**, **35d-e**, **35g**, and **35i**) generally exhibited strong AR antagonist activities (i.e.,  $\text{IC}_{50} = 0.021 \mu\text{M}$  for **35i**) but did not bind robustly to AR LBD ( $K_j > 100 \mu\text{M}$  for **35i**) and also exhibit weak degradation properties (0% for FL, SV for **35i**) as shown in Table 5. Additionally, inhibition of AR transactivation by the class III 3-substituted indazoles (compounds **35b**, **35h**, and **35i**;  $\text{IC}_{50} = 0.0267$ ,  $0.0485$ , and  $0.02097 \mu\text{M}$ , respectively) was superior to that by either enzalutamide (compound **2**) or UT-155 (compound **8**), as shown in Table 5, illustrating that our SAR-derived strategy of blocking the 2- and 3-positions of the indole B-ring was effective.

For easy-going expediency, to summarize antagonism of AR transactivation ( $\text{IC}_{50}$ ) by representative compounds (e.g., **27**, **34**, **31**, **32**, and **35**) was comparative with that of enzalutamide (compound **2**) and the indole UT-155 (compound **8**) in Figure S3.

In due course of following our previous report,<sup>13</sup> AR antagonism ( $\text{IC}_{50}$ ) evaluated on enzalutamide-resistant mutant AR-F876L (phenylalanine 876 mutated to leucine) and the Enz-Res transactivation  $\text{IC}_{50}$  of selected compounds of Class I–III is summarized by classes in Figure 6. In summary, the enzalutamide-resistant mutant AR-F876L ( $\text{IC}_{50}$ ) in Figure 5 as representative compounds (e.g., **27**, **34**, **31**, **32** and **35**) generally demonstrated to be compatible with their AR wild-type (wtAR) shown in Figure 5 and Figure S3.

We next examined the ability of selected 3-substituted indazoles in the compound **35** series to inhibit transcription of enzalutamide-resistant AR-F876L (phenylalanine 876 mutated to leucine) in cultured LNCaP cells (Figure 6), as described in the legend to Figure 6 and the Experimental section in chapter 7–14 in Supporting Information section. The results indicated that treatment of LNCaP androgen-sensitive human prostate cancer cells with increasing concentrations (1 to  $3 \mu\text{M}$ ) of enzalutamide (Enzalutamide, compound **2**) or 3-substituted indazole compounds **35a**, **35c**, and **35d** reduced expression of the mRNA encoding AR-target gene FK506 binding protein 5 (FKBP5), as shown in Figure 6.

We also evaluated levels of the mRNA that encodes prostate-specific antigen (PSA) in LNCaP cells treated with series **35** compounds. The position 2- and 3-blocked compounds **35a**, **35c** and **35d** exhibited a dose-dependent reduction in PSA (1 to  $10 \mu\text{M}$ ), as shown in Figure 6B. Finally, we examined the effect of these compounds on FKBP5 expression in LNCaP cell derivatives that are resistant to enzalutamide (EnzR). While enzalutamide (compound **2**) treatment was ineffective in these cells as expected, both parental indole UT-155 (compound **8**) and the **35** series compounds were effective in decreasing levels of FKBP5 mRNA despite the enzalutamide resistance (Figure 6C). In summary, most of compound **35** series showed inhibition of FKBP5 and PSA mRNAs in both LNCaP and enzalutamide resistance LNCaP cells.



#### 2.4. *In Vitro* Metabolic Stabilities of Class I, II, and III Derivatives in Mouse Liver Microsomes (MLM).

We measured the stability of selected class I–III derivatives using a metabolic assay in mouse liver microsomes (MLM) supplemented with the cofactors of enzymes involved in phase I and II metabolism. The half-life ( $T_{1/2}$ ) and intrinsic clearance ( $CL_{int}$ ) values shown in Table 6 were calculated as a predictor of the distribution, metabolism, and pharmacokinetic (PK) properties of these compounds.

The half-lives of most of the Class I–III derivatives were longer than that of parental indole UT-155 (compound **8**;  $T_{1/2}$  = 12.35 min). For example, the B-ring Class I derivatives with bulky carbazole groups (compounds **27b** and **27c**) exhibited  $T_{1/2}$  values of 41.77 and 39.94 min, respectively. The Class II derivatives with F-, Cl- or CN- in the 3-position of the indole B-ring (compounds **31h**, **31i**, and **31q**) exhibited relatively unfavorable *in vitro* metabolic stabilities with  $T_{1/2}$  values of 7.70, 23.44, and 12.63 min, respectively, and  $CL_{int}$  values of 8.9, 2.96, and 5.5 mL/min/mg, respectively, relative to 5.614 mL/min/mg for UT-155 (compound **8**), as shown in Table 6). Compound **31j** with a pyrido A-ring exhibited a marginal increase in  $T_{1/2}$  to 14.60 min relative to that of compound **8**, suggesting that while the pyrido group protected the A-ring from metabolism, it was primarily its B-ring that was metabolized. Compounds **31l**, **31n**, and **31o**, all of which have a 3-carbaldehyde or oxime B-ring, exhibited significantly increased half-lives ( $T_{1/2}$  = 55.0, 36.32, and 50.15 min, respectively), suggesting that the 3-position of the indole in B-ring is critical for *in vitro* metabolic stability.

The 4-F substituted B-ring indazole of compound **32a** ( $T_{1/2}$  = 13.29 min) manifested more stable elements than the parental indole UT-155 (compound **8**), although the half-lives of the two compounds were roughly comparable, whereas the CF<sub>3</sub> group on the indazole in compound **32c** dramatically decreased its metabolism ( $T_{1/2}$  = 53.71 min) and resulted in slower clearance from plasma ( $CL_{int}$  = 1.29 mL/min/mg). The B-ring indazole regioisomer, compound **32d**, also increased its stability ( $T_{1/2}$  = 35.46 min).

Finally, the 3-indazole substituted **35** series compounds, particularly the indazole dihalides in positions 3 and 4 or 3 and 5 of compounds **35b–c** and **35g**, exhibited a longer half-life in MLM. For example, the 3-methyl-5-fluoro indazole compound **35g** was more stable ( $T_{1/2}$  = 23.66 min) than UT-155 (compound **8**;  $T_{1/2}$  = 12.35 min). Compounds **35h** and **35i** with electron withdrawing groups in this position exhibited even greater stability, with  $T_{1/2}$  values of 105 min for **35h** and 120.60 min for **35i**. The 3-substituted indazole compound **35i** also exhibited improved potency in inhibiting AR transactivation ( $IC_{50}$  = 0.021  $\mu$ M), relative to UT-155 (compound **8**;  $IC_{50}$  = 0.085  $\mu$ M) or enzalutamide (compound **2**;  $IC_{50}$  = 0.216  $\mu$ M). In summary, AR binding and AR antagonistic activity of UT-155 derivatives with Class I–III B-ring substituents appear to be optimized relative to the parental indole compound **8** (Tables 4 and 5).

#### 2.5. *In Vivo* Antagonism of Compounds **31** and **35** in Rats.<sup>21,22</sup>

To examine the SAR of position 2- and 3-substituted indole B-rings in the *in vivo* test, compounds in the **31** and **35** series were selected for analysis by *in vivo* Hershberger assay

in rats (Figures 7 and 8). We selected the **31** series compounds based on their metabolic stability.

**2.5.1. Hershberger Assays in Rats with 31 Series.**—For the evaluation of *in vivo* antagonistic efficacy, intact male Sprague–Dawley rats (6–8 weeks old) were randomized into groups based on body weight and treated orally with a vehicle, 40 mg/kg/day of UT-155 (compound **8**) or 40 mg/kg/day of the indicated compound **31** derivative for 14 days.

The animals were sacrificed, their prostates and seminal vesicles were weighed, and the organ weights were normalized to body weight for each animal. The tested compounds were **31o** (pyrido A-ring and 3-oxime B-ring); **31r** (pyrido A-ring and 3-CN B-ring); **31n** (nonpyrido A-ring and 3-oxime B-ring); and **31q** (nonpyrido A-ring and 3-CN B-ring), as shown in Figure 7. Treatment of rats with molecules containing an oxime moiety in the B-ring (compounds **31o** and **31n**) exhibited relatively poor *in vivo* activity (less than 20% atrophy of prostate and seminal vesicles), relative to compound **8** (nearly 30%), as shown in Figure 7A. Despite both having cyano-substituted B-rings, treatment with compound **31r** led to greater atrophy of the prostate (weight ~4 times less than that of **31o** (Figure 7A)) but comparable effects as **31o** on the seminal vesicles (Figure 7B), while the effect of treatment with **31q** on size of the prostate and seminal vesicles were comparable with that of **31n** (Figure 7A).

**2.5.2. In Vivo Antagonism of Selected 35 Series Compounds in Rats.**—To further evaluate the *in vivo* SAR of the 3-pyrido A-ring compounds **35d** (3Cl, 5F-indazole in B-ring), **35e** (3Br, 5F-indazole), and **35g** (3CH<sub>3</sub>, 5F-indazole), we performed a Hershberger assay on intact male rats with either vehicle alone or UT-155 indole (compound **8**) as controls (Figure 8). While treatment with the indole (compound **8**) led to a change in the weight of the seminal vesicles of less than 20%, relative to the vehicle, 3-protected indazole compounds **35d**, **35e**, and **35g** caused a nearly 40% increase in atrophy of the rat AR-dependent seminal vesicles (Figure 8). In summary, the 3-substituted indazoles (**35d**, **35e**, and **35g**) exhibited robust AR antagonism *in vivo* in rats using a Hershberger assay.

## 2.6. Metabolic Study of Indole UT-155 (Compound **8**) and Its Indazole Derivative (Compound **32c**).

Compounds **32c** (indazole) and **8** (indole) were selected for exploration of the metabolic stability of the indole template, especially the 2- and 3-positions of indole UT-155 (compound **8**), by systematically eliminating metabolic soft spots in the indole nucleus. Thus, we examined the stability of indole **8** and the 2N-protected indazole **32c** in the hepatocytes (liver cells) of several species, including mouse, rat, dog, monkey, and human, to enable lead compound selection. We detected nine metabolites (M1–M9) of indole compound **8** that displayed oxidation and/or glycosylation (Table 7). By comparison, the protected mode of indazole **32c** resulted in detection of fewer metabolites (M1–M5), suggesting that it was more stable than indole **8** (Table 7).

**2.6.1. Provisional Biotransformation Pathways of UT-155 (Compound **8**).**—We detected evidence for four major metabolic pathways in the degradation of compound **8**

(Table 7, panel A), as follows. We detected 1) oxidation in metabolites M1, M3, M4, M7, and M9; 2) O-glucuronidation in metabolites M2 and M5; 3) O-sulfation in metabolite M6; and 4) direct glucuronidation in metabolite M8. The putative structures of these metabolites and their relative abundance in each species by peak area are shown in Table 7, panel A. The most abundant metabolite in human liver cells (M8) was also observed in monkey hepatocytes but not in those of rat, dog, or mouse. The other major metabolites detected in human hepatocytes (M4, M5) were also detected in all other species assessed.

M1 and M6 were the major metabolites in rat hepatocytes; M2 in rat, dog, and mouse; M7 in dog and mouse; and M9 in monkey; all of these metabolites also observed at varying abundance in human hepatocytes. M3 was a major metabolite in mouse hepatocytes but was not detected in human hepatocytes.

**2.6.2. Provisional Biotransformation Pathways of 32c.**—We also detected evidence for four major metabolic pathways in the degradation of compound **32c** (Table 7, panel B), as follows. We detected 1) dihydro-diols in M1 and M2; 2) O-sulfation in M3; 3) O-glucuronidation in M4; and 4) oxidation in M5. The putative structures of these metabolites are shown in Table 7, panel B, and their relative abundance in each species by peak area is shown in Table 9. The three most abundant metabolites in human hepatocytes (M4, M3, and M1) were observed in all other species evaluated. M2 was a major metabolite in monkey hepatocytes and M5 in dog hepatocytes, both of which were observed in human hepatocytes.

### 3. CONCLUSIONS AND DISCUSSION

In our continued effort to discover bioactive small molecules that antagonize the AR activity for treatment of advanced PC, we designed and evaluated more than 50 new compounds with alteration of the 2- and/or 3-positions in the indole B-ring of compound UT-155 (compound **8**) that can be divided into three structural classes. The obtained results are summarized in Table 10.

The Class II derivative, compound **32c**, that contained an indazole at position 2 of the indole B-ring exhibited a dramatic improvement in *in vitro* metabolic stability ( $T_{1/2} = 53.71$  min), which is four times more stable than the parental indole compound **8**, as shown in Table 6. This result suggested that the 2- and 3-positions of the parental indole B-ring in compound **8** were the most metabolically labile. This was also supported by the results of the metabolic assessment of compound **32c**, which showed that there was comparatively little metabolism of the protected 2- and 3-positions of compound **32c** and no glycosylation on the B-ring hydroxyl group (Table 7, panel B and Table 9).

By comparison, metabolic assessment of parental indole compound **8** suggested that the 2- and 3-positions of the B-ring were metabolized by oxidation/glycosylation and sulfonylation/glycosylation on the hydroxyl of compound **8** to yield the major metabolites M1–M9 (Table 7, panel A and Table 8). We further showed that the presence of a pyrido group on the indole A ring, for example in compound **20**, strengthened the antagonistic effect for enzalutamide-resistant AR relative to that of the parental indole compound **8** (IC<sub>50</sub>

= 0.027  $\mu\text{M}$  for compound 20; 0.085  $\mu\text{M}$  for compound 8), although the two compounds exhibited similar stability (half-life) and similar binding affinity ( $K_i$ ) for the AR ligand binding domain (LBD), as shown in Table 1.

When we combined the A-ring pyrido moiety (in compound 20) with the 3-substituted indazole B-ring (in compound 32c), we discovered that the resulting compound 35i exhibited four times the potency in antagonizing AR transactivation ( $\text{IC}_{50} = 0.021 \mu\text{M}$ , as shown in Table 5) and ten times greater metabolic stability ( $T_{1/2} = 120.6 \text{ min}$ , as shown in Table 7) than the parental indole compound 8, and this activity was enzalutamide resistant. Compounds in the 31, 32, and 35 series exhibited improved antagonism of AR transactivation ( $\text{IC}_{50}$ ) and greater stability than compound 8 and were also able to degrade both FL and SV versions of AR (Tables 4 and 5). To determine the selectivity of this scaffold we performed a proteomics analysis with UT-155 in AR-negative PC-3 cells. UT-155 did not alter the proteome, suggesting that the scaffold selectively modulates AR and androgenic pathways and does not have off-target effects.

In summary, the current study explored the strategy of blocking the 2- and 3-positions of the B-ring indole of UT-155 (compound 8) in hopes of improving its stability. The success of this strategy was highlighted by our findings that many of the resulting compounds demonstrated not only increased stability but also strengthened *in vitro* (e.g., antagonism, SARD, and antiproliferative assays)/*in vivo* (e.g., xenografts) activities as AR antagonists that retained their functionalities even against enzalutamide-resistant forms of AR. Collectively, this metabolism-guided study could be a stepping stone to the discovery of potent AR antagonist-targeted small molecules.

## 4. EXPERIMENTAL SECTION

### 4.1. General Chemistry Methods.

All solvents and chemicals used for synthesis were purchased from Sigma-Aldrich Chemical Co. (Burlington, MA), Fisher Scientific (Pittsburgh, PA), Matrix Scientific (Columbia, SC), Ambeed Inc. (Arlington Heights, IL), AURUM Pharmatech (Franklin Park, NJ), Combi-Blocks Inc. (San Diego, CA), and others and were used without further purification. All moisture-sensitive reactions were performed under an argon atmosphere. Analytical thin-layer chromatography (TLC) was performed on precoated silica gel plates (Merck Kieselgel 60 F<sub>254</sub> layer thickness 0.25 mm). NMR spectra were obtained on a Bruker Avance III 400 spectrometer (Billerica, MA). Chemical shifts are reported in parts per million (ppm) relative to tetramethylsilane (TMS) in chloroform ( $\text{CDCl}_3$ ), Acetone- $d_6$  or dimethyl sulfoxide (DMSO)- $d_6$ . The structures of synthesized compounds were also assigned using  $^1\text{H}$ - $^1\text{H}$  2D-COSY and 2D-NOESY NMR analytical methods. Flash column chromatography was performed using silica gel (230–400 mesh, Merck) columns. Mass spectral data was collected on a Bruker Esquire liquid chromatography/mass spectrometry (LCMS) system (Bruker Daltonics, Billerica, MA) equipped with an electrospray/ion trap instrument in positive and negative ion modes (ESI Source Solutions, LLC, Woburn, MA). The purity of the final compounds was analyzed by an Agilent 1100 high-pressure liquid chromatography (HPLC) system (Santa Clara, CA). HPLC conditions: 45% acetonitrile at flow rate of 1.0 mL/min using a LUNA 5  $\mu\text{m}$  C18 100A column (250  $\times$  4.60 mm; Phenomenex, Torrance,

CA) at ambient temperature. UV detection was set at 340 or 245 nm. Purities of the compounds were determined by careful integration of areas for all peaks detected and determined as >95% for all compounds evaluated for biological activity against PC.

#### 4.2. Metabolic Study of Compounds **8** and **32c**.

This study was conducted by Covance Laboratories Inc. (Covance; Madison, WI), in accordance with the protocol and standard operating procedures (SOPs) from Covance.

**Biotransformation in Hepatocytes.**—The biotransformation of test articles was assessed by incubation of mouse, rat, dog, monkey, and human hepatocytes with 10  $\mu$ M solutions of compounds **8** or **32c** for 0 and 120 min. The three major metabolites in the 120 min samples were identified for each species. The major metabolites for the human cells were assessed in all preclinical species tested, while the major metabolites for each preclinical species were assessed in human hepatocytes, but not in hepatocytes from other species. Due to saturation of the parent LCMS signal, the quantitation of the metabolites as a percentage of the parent compound was not possible and was instead limited to the metabolite peak area.

**Experimental Assessment in Cultured Hepatocytes.**—Metabolic biotransformation of the test articles was assessed *in vitro* using cultured mouse, rat, dog, monkey, and human hepatocytes. Each of nine test articles (10  $\mu$ M each) were incubated separately with approximately  $1 \times 10^6$  hepatocytes/mL, suspended in Williams' Medium E, at 37 °C in 5% CO<sub>2</sub>. Parallel cultures were terminated after 0 or 120 min by the addition of acetonitrile, and the samples were stored frozen at -20 °C until time of analysis. All incubations were conducted in duplicate. Metabolites of five selected AR antagonists were characterized using quantitative liquid chromatography tandem mass spectrometry (LC-MS/MS). Metabolite structures were proposed based on mass accuracy and their ion fragmentation.

#### 4.3. General Synthetic Procedures.

**4.3.1. Synthetic Method A<sup>13</sup> (for Compounds **27a–27 e**, **31a–31b**, **31h–31s**, **32c–32d**, **34a–34 h**, and **35a–35g**).**—Under an argon atmosphere, a 60% dispersion of NaH (228 mg, 5.7 mmol) in mineral oil was added to 30 mL of anhydrous tetrahydrofuran (THF) in a dry two-necked round-bottom flask equipped with a dropping funnel, and the resulting solution was stirred in an ice–water bath for 30 min (Scheme 1). Separately, 2.84 mmol of substituted compound **25** (or compounds **28**, **29**, **30**, **32**, or **33**) was dissolved in 100 mL THF, and the resulting solution was added to the flask through the dropping funnel under an argon atmosphere and stirred overnight at RT. After adding 1 mL of H<sub>2</sub>O, the reaction mixture was condensed under reduced pressure, dispersed into 50 mL of ethyl acetate (EtOAc), washed twice with 50 mL H<sub>2</sub>O, evaporated, dried over anhydrous MgSO<sub>4</sub>, and evaporated to dryness. The mixture was purified with flash column chromatography as an EtOAc/hexane eluent to produce the desired compounds.

**4.3.2. Synthetic Method B (for Compound **31c**).**—To a dry, nitrogen-purged 50 mL round-bottom flask, *R*-bromo amide (compound **23**, 1 mmol), substituted benzimidazole or indazole (1 mmol), and K<sub>2</sub>CO<sub>3</sub> (415 mg, 3 mmol) were dissolved into 10 mL of

DMF. The mixture was heated to 80 °C for 2 h, then cooled to RT. The mixture was concentrated under reduced pressure, poured into 10 mL of H<sub>2</sub>O, and extracted 3 times with EtOAc. The organic layer was dried over anhydrous MgSO<sub>4</sub>, concentrated, purified by flash chromatography on a silica gel column, and eluted with EtOAc to produce the desired product.

**4.3.3. Synthetic Method C (for Compounds 31d–31g, 32a, and 32b).**—Under an argon atmosphere, 1.5 mL of lithium bis(trimethylsilyl)amide (1 mmol; 1 M solution in THF) was slowly added to a solution of substituted-benzimidazole (compound **29**; 1 mmol in 10 mL THF) at –78 °C and stirred for 30 min. A solution of aryl bromide (compound **23**, 1 mmol in 5 mL THF) was added dropwise to the solution. The reaction mixture was stirred at –78 °C for 30 min, then at RT overnight. The reaction was quenched by the addition of 10 mL of a saturated NH<sub>4</sub>Cl solution. The mixture was concentrated under reduced pressure and dispersed into excess EtOAc, dried over Na<sub>2</sub>SO<sub>4</sub>, concentrated, and purified by flash column chromatography (EtOAc/hexane) to produce the target product.

**4.3.4. Synthetic Method D<sup>37</sup> (for Compounds 31n–31p).**—Hydroxylamine hydrochloride (for compounds **31n** or **31o**) or acetohydrazide (1.5 mmol for compound **31p**) was added to a solution of compound **31l** or **31m** (0.69 mmol in 5 mL pyridine). The solution was stirred overnight at RT before being evaporated to dryness. The residue was dissolved in 20 mL of EtOAc, and 10 mL of H<sub>2</sub>O was added to the solution. The residue was filtered and washed with H<sub>2</sub>O or purified with flash column chromatography and eluted in EtOAc/hexane to produce the desired compounds.

#### 4.4. Synthesis and Analysis of Compounds 26, 27(a–e), 28, 31(a–s), 32(a–d), 34(a–h), and 35(a–k).

**(S)-N-(4-Cyano-3-(trifluoromethyl)phenyl)-3-(2,3-dioxindolin-1-yl)-2-hydroxy-2-methylpropanamide (26).**—To a dry, nitrogen-purged 100 mL round-bottom flask under an argon atmosphere was added a mixture of indoline-2,3-dione (147 mg, 10.0 mmol), (*R*)-3-bromo-*N*-(4-cyano-3-(trifluoromethyl) phenyl)-2-hydroxy-2-methylpropanamide (351 mg, 10.0 mmol), and K<sub>2</sub>CO<sub>3</sub> (14.5 mmol, 277 mg) in 5 mL of DMF and stirred vigorously at RT for 12 h. The reaction mixture was poured into 50 mL of H<sub>2</sub>O and extracted 3 times with 10 mL of EtOAc, washed with brine (saturated NaCl in H<sub>2</sub>O), aqueous NH<sub>4</sub>Cl, and H<sub>2</sub>O. The EtOAc extract was dried over anhydrous MgSO<sub>4</sub>, concentrated under reduced pressure, and purified by flash column chromatography using EtOAc/hexane (1:1, v/v) as an eluent to produce compound **26** as a brown gel (yield 34%). UV  $\lambda_{\text{max}}$  197.45, 270.45 nm; HPLC (45% acetonitrile):  $t_{\text{R}}$  3.18 min, purity 97.82%; MS (ESI)  $m/z$  416.2 [M – H]<sup>–</sup>; <sup>1</sup>H NMR (CDCl<sub>3</sub>, 400 MHz)  $\delta$  9.16 (bs, 1H, NH), 8.09 (d,  $J$  = 1.6 Hz, 1H), 7.92 (d,  $J$  = 8.4, 1.6 Hz, 1H), 7.79 (d,  $J$  = 8.4 Hz, 1H), 6.91 (t,  $J$  = 8.4 Hz, 2H), 6.60 (d,  $J$  = 8.4 Hz, 1H), 6.56 (d,  $J$  = 8.4 Hz, 1H), 4.52 (bs, OH), 3.84 (d,  $J$  = 13.6 Hz, 1H), 3.25 (d,  $J$  = 13.6 Hz, 1H), 1.57 (s, 3H); <sup>13</sup>C NMR (CDCl<sub>3</sub>, 100 MHz)  $\delta$  173.9, 158.5, 156.2, 142.7, 141.4, 135.8, 133.9 (q,  $J$  = 33 Hz), 123.4, 121.8, 120.7, 117.3 (q,  $J$  = 5 Hz), 116.4, 116.3, 116.1, 115.9, 115.5, 104.6, 60.5, 21.1; <sup>19</sup>F NMR (CDCl<sub>3</sub>, 400 MHz)  $\delta$  –62.21.



**(S)-3-(9H-Carbazol-9-yl)-N-(4-cyano-3-(trifluoromethyl)phenyl)-2-hydroxy-2-methylpropanamide (27a).**—Synthetic Method A was used to produce compound **27a** (yield 76%). MS (ESI) 436.1 [M – H]<sup>–</sup>; <sup>1</sup>H NMR (400 MHz, CDCl<sub>3</sub>) δ 8.81 (bs, 1H, NH), 8.09–8.06 (m, 2H), 7.84 (d, *J* = 1.6 Hz, 1H), 7.77–7.71 (m, 2H), 7.55 (d, *J* = 8.4 Hz, 2H), 7.45–7.39 (m, 2H), 7.24–7.26 (m, 2H), 4.80 (d, *J* = 15.2 Hz, 1H), 4.62 (d, *J* = 15.2 Hz, 1H), 2.57 (bs, 1H, OH), 1.69 (s, 3H).

**(S)-3-(9H-Carbazol-9-yl)-N-(3-chloro-4-cyanophenyl)-2-hydroxy-2-methylpropanamide (27b).**—Synthetic Method A was used to produce compound **27b** (yield 77%). MS (ESI) *m/z* 402.3 [M – H]<sup>–</sup>; <sup>1</sup>H NMR (400 MHz, CDCl<sub>3</sub>) δ 8.75 (bs, 1H, NH), 8.08 (d, *J* = 7.6 Hz, 2H), 7.78 (d, *J* = 1.6 Hz, 1H), 7.56–7.54 (m, 3H), 7.44 (t, *J* = 7.6 Hz, 2H), 7.37 (dd, *J* = 8.8, 1.8 Hz, 1H), 7.27–7.25 (m, 2H), 4.78 (d, *J* = 15.6 Hz, 1H), 4.63 (d, *J* = 15.6 Hz, 1H), 2.65 (bs, 1H, OH), 1.66 (s, 3H).

**(S)-N-(4-Cyano-3-(trifluoromethyl)phenyl)-3-(3-fluoro-9H-carbazol-9-yl)-2-hydroxy-2-methylpropanamide (27c).**—Synthetic Method A was used to produce compound **27c** as a white solid (yield 73.5%). Mass (ESI) 453.9 [M – H]<sup>–</sup>; (ESI): 478.1[M + Na]<sup>+</sup>; <sup>1</sup>H NMR (400 MHz, DMSO-*d*<sub>6</sub>) δ 10.36 (s, 1H, NH), 8.25 (d, *J* = 1.6 Hz, 1H, ArH), 8.12–8.09 (m, 2H, ArH), 8.04 (d, *J* = 8.8 Hz, 1H, ArH), 7.95 (dd, *J* = 9.2 Hz, *J* = 2.1 Hz, 1H, ArH), 7.66 (t, *J* = 4.8 Hz, 1H, ArH), 7.64 (s, 1H, ArH), 7.37 (dt, *J* = 9.2 Hz, *J* = 1.2 Hz, 1H, ArH), 7.20 (td, *J* = 9.2 Hz, *J* = 2.0 Hz, 1H, ArH), 7.13 (t, *J* = 8.0 Hz, 1H, ArH), 6.34 (s, 1H, OH), 4.70 (d, *J* = 14.8 Hz, 1H, CH), 4.55 (d, *J* = 14.8 Hz, 1H, CH), 1.52 (s, 3H, CH<sub>3</sub>).

**(S)-N-(3-Chloro-4-cyanophenyl)-3-(3-fluoro-9H-carbazol-9-yl)-2-hydroxy-2-methylpropanamide (27d).**—Synthetic Method A was used to produce compound **27d** as a white solid/needles (yield 98%). Mass (ESI) 420.1 [M – H]<sup>–</sup>; (ESI): 444.1 [M + Na]<sup>+</sup>; <sup>1</sup>H NMR (400 MHz, DMSO-*d*<sub>6</sub>) δ 10.20 (s, 1H, NH), 8.12 (d, *J* = 7.6 Hz, 1H, ArH), 8.05 (d, *J* = 2.0 Hz, 1H, ArH), 7.96 (dd, *J* = 9.2, 2.0 Hz, 1H, ArH), 7.86 (d, *J* = 8.8 Hz, 1H, ArH), 7.80 (dd, *J* = 8.4, 2.0 Hz, 1H, ArH), 7.69–7.66 (m, 2H, ArH), 7.41 (t, *J* = 8.0, 1H, ArH), 7.24 (dt, *J* = 9.6, 2.4 Hz, 1H, ArH), 7.16 (t, *J* = 7.2 Hz, 1H, ArH), 6.34 (s, 1H, OH), 4.70 (d, *J* = 15.2 Hz, 1H, CH), 4.54 (d, *J* = 15.2 Hz, 1H, CH), 1.52 (s, 3H, CH<sub>3</sub>).

**(S)-N-(4-Cyano-3-(trifluoromethyl)phenyl)-3-(3,6-difluoro-9H-carbazol-9-yl)-2-hydroxy-2-methylpropanamide (27e).**—Synthetic Method A was used to produce compound **27e** as a white solid (yield 85.8%). Mass (ESI) 471.9 [M – H]<sup>–</sup>; 496.1 [M + Na]<sup>+</sup>; <sup>1</sup>H NMR (400 MHz, DMSO-*d*<sub>6</sub>) δ 10.33 (s, 1H, NH), 8.22 (d, *J* = 1.6 Hz, 1H, ArH), 8.11 (dd, *J* = 8.8, 2.0 Hz, 1H, ArH), 8.05 (d, *J* = 8.8 Hz, 1H, ArH), 7.98 (d, *J* = 2.4 Hz, 1H, ArH), 7.96 (d, *J* = 2.4 Hz, 1H, ArH), 7.68–7.65 (m, 2H, ArH), 7.27–7.22 (m, 2H, ArH), 6.36 (s, 1H, OH), 4.72 (d, *J* = 15.2 Hz, 1H, CH), 4.54 (d, *J* = 15.2 Hz, 1H, CH), 1.53 (s, 3H, CH<sub>3</sub>).

**3,5-Difluoro-1H-indole (28).**—Selectfluor (872 mg, 2.0 mmol, 2.0 equiv) as a fluorine donor, Li<sub>2</sub>CO<sub>3</sub> (296 mg, 4.0 mmol, 4.0 equiv), dichloromethane (3.3 mL), and H<sub>2</sub>O (1.7 mL) were added to a 50 mL round-bottom flask containing a magnetic stir bar. Carboxylic acid (1.0 mmol, 1.0 equiv) was added, and the reaction mixture was stirred for 2 h in an

ice bath. The reaction mixture was diluted with 40 mL of H<sub>2</sub>O and extracted twice with 20 mL of dichloromethane (DCM). The combined organic extracts were washed with brine, dried over anhydrous sodium sulfate, and concentrated *in vacuo*. The crude product was purified by flash column chromatography (*n*-hexane:DCM = 2:1) to produce compound **28** as a dark brown oil (yield 68%). MS (ESI) *m/z* 154.83[M + H]<sup>+</sup>; 152.03 [M – H]<sup>–</sup>; <sup>1</sup>H NMR (CDCl<sub>3</sub>, 400 MHz) δ 7.86 (bs, 1H, NH), 7.25 (dd, *J* = 9.2, 2.4 Hz, 1H), 7.20–7.16 (m, 1H), 6.97 (t, *J* = 2.6 Hz, 1H), 6.93 (dd, *J* = 9.2, 2.4 Hz, 1H), ; <sup>19</sup>F NMR (CDCl<sub>3</sub>) δ –123.99 (*d*, *J*<sub>F–F</sub> = 2.8 Hz), –174.74 (*d*, *J*<sub>F–F</sub> = 4.0 Hz).

**(S)-N-(4-Cyano-3-(trifluoromethyl)phenyl)-3-(5,6-difluoro-1H-benzo[d]imidazol-1-yl)-2-hydroxy-2-methylpropanamide (31a).**—Synthetic

Method A was used to produce compound **31a** as a white solid (yield 12.6%). Mass (ESI) 422.7 [M – H]<sup>–</sup>; 447.0 [M + Na]<sup>+</sup>; <sup>1</sup>H NMR (400 MHz, DMSO-*d*<sub>6</sub>) δ 10.36 (s, 1H, NH), 8.25 (d, *J* = 2.0 Hz, 1H, ArH), 8.21 (s, 1H, ArH), 8.14 (dd, *J* = 8.8, 2.0 Hz, 1H, ArH), 8.06 (d, *J* = 8.8 Hz, 1H, ArH), 7.43–7.40 (m, 1H, ArH), 7.26–7.19 (m, 1H, ArH), 6.51 (s, 1H, OH), 4.65 (d, *J* = 14.8 Hz, 1H, CH), 4.41 (d, *J* = 14.8 Hz, 1H, CH), 1.42 (s, 3H, CH<sub>3</sub>).

**(S)-N-(4-Cyano-3-(trifluoromethyl)phenyl)-3-(5,6-difluoro-1H-benzo[d]imidazol-2-yl)-2-hydroxy-2-methylpropanamide (31b).**—Synthetic

Method A was used to produce compound **31b** as a white solid (yield 28.4%). Mass (ESI) 422.7 [M – H]<sup>–</sup>; 447.0 [M + Na]<sup>+</sup>; <sup>1</sup>H NMR (400 MHz, DMSO-*d*<sub>6</sub>) δ 10.44 (s, 1H, NH), 8.36 (d, *J* = 2.0 Hz, 1H, ArH), 8.17 (dd, *J* = 8.4, 2.0 Hz, 1H, ArH), 8.11 (s, 1H, ArH), 8.07 (d, *J* = 8.4 Hz, 1H, ArH), 7.44–7.41 (m, 1H, ArH), 7.21–7.14 (m, 1H, ArH), 6.54 (s, 1H, OH), 4.62 (d, *J* = 14.4 Hz, 1H, CH), 4.52 (d, *J* = 14.4 Hz, 1H, CH), 1.41 (s, 3H, CH<sub>3</sub>).

**(S)-N-(3-Chloro-4-cyanophenyl)-3-(4-fluoro-1H-benzo[d]imidazol-1-yl)-2-hydroxy-2-methylpropanamide (31c).**—Synthetic Method B was used

to produce compound **31c** (yield 63%). HRMS (ESI) *m/z* calcd for C<sub>18</sub>H<sub>15</sub>ClF<sub>4</sub>N<sub>4</sub>O<sub>2</sub>: 373.0868. Found: 373.0878 [M + H]<sup>+</sup>; <sup>1</sup>H NMR (Acetone-*d*<sub>6</sub>, 400 MHz) δ 9.77 (bs, 1H, NH), 8.16 (d, *J* = 1.6 Hz, 1H), 8.04 (s, 1H), 7.83 (dd, *J* = 8.4, 1.6 Hz, 1H), 7.75 (d, *J* = 1.6 Hz, 1H), 7.44 (d, *J* = 4.8 Hz, 1H), 7.18 (m, 1H), 6.99 (dd, *J* = 11.6, 8.0 Hz, 1H), 5.83 (bs, 1H, OH), 4.78 (d, *J* = 14.4 Hz, 1H), 4.69 (d, *J* = 14.4 Hz, 1H), 1.56 (s, 3H).

**(S)-N-(4-Cyano-3-(trifluoromethyl)phenyl)-3-(7-fluoro-1H-benzo[d]imidazol-1-yl)-2-hydroxy-2-methylpropanamide (31d).**—Synthetic Method C was used

to produce compound **31d** (and compound **31e**, see below) as a white solid (total yield of compounds **31d** and **31e**, 70%; yield of compound **31d**, 30%). HRMS (ESI) *m/z* calcd for C<sub>19</sub>H<sub>15</sub>F<sub>4</sub>N<sub>4</sub>O<sub>2</sub>: 457.1131. Found: 457.1126 [M + H]<sup>+</sup>; <sup>1</sup>H NMR (CDCl<sub>3</sub>, 400 MHz) δ 9.14 (bs, 1H, NH), 8.08 (s, 1H), 7.96 (s, 1H), 7.82 (d, *J* = 8.2 Hz, 1H), 7.73 (d, *J* = 8.4 Hz, 1H), 7.72 (d, *J* = 8.4 Hz, 1H), 7.42 (d, *J* = 8.8 Hz, 1H), 7.23 (m, 1H), 7.67 (dd, *J* = 10.0, 7.6 Hz, 1H), 6.67 (bs, 1H, OH), 4.96 (d, *J* = 13.6 Hz, 1H), 4.54 (d, *J* = 13.6 Hz, 1H), 1.54 (s, 3H); <sup>19</sup>F NMR (CDCl<sub>3</sub>, 400 MHz) δ –62.22, –116.56.

**(S)-N-(4-Cyano-3-(trifluoromethyl)phenyl)-3-(4-fluoro-1H-benzo[d]imidazol-1-yl)-2-hydroxy-2-methylpropanamide (31e).**—Synthetic Method C was used to

produce compound **31e** (and compound **31d**, see above) as a white solid (total yield of compounds **31d** and **31e**, 70%; yield of compound **31e**, 40%). HRMS (ESI)  $m/z$  calcd for  $C_{19}H_{15}F_4N_4O_2$ : 457.1131. Found: 457.1137  $[M + H]^+$ ;  $^1H$  NMR ( $CDCl_3$ , 400 MHz)  $\delta$  9.10 (bs, 1H, *NH*), 8.11 (s, 1H), 7.79 (s, 1H), 7.75–7.71 (m, 2H), 7.38 (m, 1H), 7.31–7.26 (m, 1H), 6.81 (t,  $J = 8.0$  Hz, 1H), 6.01 (bs, 1H, OH), 4.93 (d,  $J = 14.0$  Hz, 1H), 4.44 (d,  $J = 14.0$  Hz, 1H), 1.53 (s, 3H);  $^{19}F$  NMR ( $CDCl_3$ , 400 MHz)  $\delta$  –62.22, –117.60.

**(S)-N-(4-Cyano-3-(trifluoromethyl)phenyl)-2-hydroxy-2-methyl-3-(4-(trifluoromethyl)-1H-benzo[d]imidazol-1-yl) propanamide (31f).**—Synthetic Method C was used to produce compound **31f** (and compound **31g**, see below) as a light yellowish solid (total yield of compounds **31f** and **31g**, 66%; yield of compound **31f**, 31.9%). The structure of the product was determined using 2D NMR (NOESY). HRMS (ESI)  $m/z$  calcd for  $C_{20}H_{14}F_6N_4O_2$ : 457.1099  $[M + H]^+$ . Found: 457.1090  $[M + H]^+$ ;  $^1H$  NMR ( $CDCl_3$ , 400 MHz)  $\delta$  9.32 (bs, 1H, *NH*), 8.26 (s, 1H), 8.12 (d,  $J = 2.0$  Hz, 1H), 7.99 (dd,  $J = 8.4, 2.0$  Hz, 1H), 7.85 (d,  $J = 8.4$  Hz, 1H), 7.77 (d,  $J = 8.0$  Hz, 1H), 7.665 (d,  $J = 8.0$  Hz, 1H), 7.29 (t,  $J = 8.0$  Hz, 1H), 5.92 (bs, 1H, OH), 4.94 (d,  $J = 15.2$  Hz, 1H), 4.68 (d,  $J = 15.2$  Hz, 1H), 1.48 (s, 3H);  $^{19}F$  NMR ( $CDCl_3$ , 400 MHz)  $\delta$  –55.42, –62.14.

**(S)-N-(4-Cyano-3-(trifluoromethyl)phenyl)-2-hydroxy-2-methyl-3-(7-(trifluoromethyl)-1H-benzo[d]imidazol-1-yl) propanamide (31g).**—Synthetic Method C was used to produce compound **31g** (and compound **31f**, see above) as a light yellowish solid (total yield of compounds **31f** and **31g**, 66%; yield of compound **31g**, 34%). The structure of the product was determined using 2D NMR (NOESY). HRMS (ESI)  $m/z$  calcd for  $C_{20}H_{14}F_6N_4O_2$ : 457.1099  $[M + H]^+$ . Found: 457.1094  $[M + H]^+$ ;  $^1H$  NMR ( $CDCl_3$ , 400 MHz)  $\delta$  9.16 (bs, 1H, *NH*), 8.07 (s, 1H), 7.95 (bs, 1H), 7.76 (d,  $J = 1.6$  Hz, 1H), 7.73 (d,  $J = 8.0$  Hz, 1H), 7.55 (d,  $J = 8.0$  Hz, 1H), 7.34 (t,  $J = 8.0$  Hz, 1H), 6.37 (bs, 1H, OH), 4.70 (d,  $J = 14.4$  Hz, 1H), 4.48 (d,  $J = 14.4$  Hz, 1H), 1.58 (s, 3H);  $^{19}F$  NMR ( $CDCl_3$ , 400 MHz)  $\delta$  –60.52, –62.29.

**(S)-N-(4-Cyano-3-(trifluoromethyl)phenyl)-3-(3,5-difluoro-1H-indol-1-yl)-2-hydroxy-2-methylpropanamide (31h).**—Synthetic Method A was used to produce compound **31h** as a white powder (yield 53%). HPLC (45% acetonitrile):  $t_R$  2.77 min, purity 99.06%. UV ( $\lambda_{max}$ ) 196.45, 270.45 nm; MS (ESI)  $m/z$  423.20  $[M + H]^+$ ; 422.02  $[M - H]^-$ ;  $C_{20}H_{15}F_5N_3O_2$  424.1084  $[M + H]^+$ ; 424.1065  $[M + H]^+$ ;  $^1H$  NMR ( $CDCl_3$ , 400 MHz)  $\delta$  8.80 (bs, 1H, *NH*), 7.89 (d,  $J = 1.6$  Hz, 1H), 7.77 (dd,  $J = 8.4, 1.6$  Hz, 1H), 7.74 (d,  $J = 8.4$  Hz, 1H), 7.33–7.29 (m, 1H), 7.20 (dd,  $J = 9.0, 2.4$  Hz, 1H), 6.99 (t,  $J = 2.8$  Hz, 1H), 6.97 (td,  $J = 9.0, 2.4$  Hz, 1H), 4.56 (d,  $J = 14.8$  Hz, 1H), 4.24 (d,  $J = 14.8$  Hz, 1H), 2.57 (s, OH), 1.61 (s, 3H);  $^{19}F$  NMR ( $CDCl_3$ )  $\delta$  –62.25, –123.48 (d,  $J_{F-F} = 3.2$  Hz), –173.54 (d,  $J_{F-F} = 2.8$  Hz).

**(S)-3-(3-Chloro-5-fluoro-1H-indol-1-yl)-N-(4-cyano-3-(trifluoromethyl)phenyl)-2-hydroxy-2-methylpropanamide (31i).**—Synthetic Method A was used to produce compound **31i** as a white solid (yield 58%). HPLC (45% acetonitrile):  $t_R$  2.89 min, purity 99.06%; UV ( $\lambda_{max}$ ) 196.45, 270.45 nm; MS (ESI)  $m/z$   $C_{20}H_{15}ClF_4N_3O_2$ : 440.0789  $[M + H]^+$ ; 440.0797  $[M + H]^+$ ;  $^1H$  NMR ( $CDCl_3$ , 400 MHz)  $\delta$  8.76 (bs, 1H, *NH*), 7.86 (s, 1H), 7.78–7.73 (m, 2H), 7.34 (dd,  $J = 9.2, 4.0$  Hz, 1H), 7.29 (dd,  $J = 8.8, 2.4$  Hz, 1H),

7.17 (s, 1H), 6.97 (td,  $J=9.2, 2.4$  Hz, 1H), 4.58 (d,  $J=14.8$  Hz, 1H), 4.28 (d,  $J=14.8$  Hz, 1H), 2.64 (s, OH), 1.61 (s, 3H);  $^{19}\text{F}$  NMR ( $\text{CDCl}_3$ )  $\delta$  -62.25, -12.76.

**(S)-N-(6-Cyano-5-(trifluoromethyl)pyridin-3-yl)-3-(5-fluoro-1H-indol-1-yl)-2-hydroxy-2-methylpropanamide (31j).**—Synthetic Method A was used

to produce compound **31j** (yield 83%). MS (ESI)  $m/z$  407.20  $[\text{M} + \text{H}]^+$ ; 405.02  $[\text{M} - \text{H}]^-$ ; HRMS (ESI)  $m/z$  calcd for  $\text{C}_{19}\text{H}_{14}\text{F}_4\text{N}_4\text{O}_2$ : 407.1131  $[\text{M} + \text{H}]^+$ . Found: 407.1128  $[\text{M} + \text{H}]^+$ ;  $^1\text{H}$  NMR ( $\text{CDCl}_3$ , 400 MHz)  $\delta$  8.85 (bs, 1H,  $\text{NH}$ ), 8.58 (d,  $J=2.0$  Hz, 1H), 8.51 (s, 1H), 7.33 (dd,  $J=8.8, 4.0$  Hz, 1H), 7.19 (d,  $J=2.4$  Hz, 1H), 7.17 (d,  $J=2.8$  Hz, 1H), 6.92 (m, 1H), 6.45 (d,  $J=2.8$  Hz, 1H), 4.64 (d,  $J=15.2$  Hz, 1H), 4.33 (d,  $J=15.2$  Hz, 1H), 2.93 (bs, 1H, OH), 1.64 (s, 3H).  $^{19}\text{F}$  NMR ( $\text{CDCl}_3$ , 400 MHz)  $\delta$  -62.08, -125.26.

**(S)-Ethyl 1-(3-((4-cyano-3-(trifluoromethyl) phenyl) amino)-2-hydroxy-2-methyl-3-oxopropyl)-5-fluoro-1H-indole-3-carboxylate (31k).**—Synthetic Method A

was used to produce compound **31k** as a yellowish solid (yield 63%). The structure of the product was determined using 2D NMR (COSY and NOESY). MS (ESI)  $m/z$  476.31  $[\text{M} - \text{H}]^-$ ; 500.26  $[\text{M} + \text{Na}]^+$ ; LCMS (ESI)  $m/z$  calcd for  $\text{C}_{23}\text{H}_{19}\text{F}_4\text{N}_3\text{O}_4$ : 476.1390  $[\text{M} - \text{H}]^-$ . Found: 476.1301  $[\text{M} - \text{H}]^-$ ;  $^1\text{H}$  NMR ( $\text{CDCl}_3$ , 400 MHz)  $\delta$  8.90 (bs, 1H,  $\text{NH}$ ), 7.98 (s, 1H), 7.88 (d,  $J=1.6$  Hz, 1H), 7.77–7.73 (m, 2H), 7.65 (dd,  $J=9.4, 2.6$  Hz, 1H), 7.42 (dd,  $J=9.4, 4.0$  Hz, 1H), 6.99 (dt,  $J=8.8, 2.6$  Hz, 1H), 4.66 (d,  $J=14.8$  Hz, 1H), 4.39 (d,  $J=14.8$  Hz, 1H), 4.17 (q,  $J=7.0$  Hz, 2H), 4.00 (s, OH), 1.68 (s, 3H), 1.38 (t,  $J=7.0$  Hz, 3H);  $^{19}\text{F}$  NMR ( $\text{CDCl}_3$ , 400 MHz)  $\delta$  -62.26, -120.93.

**(S)-N-(4-Cyano-3-(trifluoromethyl)phenyl)-3-(5-fluoro-3-formyl-1H-indol-1-yl)-2-hydroxy-2-methylpropanamide (31l).**—Synthetic Method A was used to produce

compound **31l** as a yellowish solid (yield 73%; purity 99.14%). The structure of the product was determined using 2D NMR (COSY and NOESY). UV max 195.45, 265.45; MS (ESI)  $m/z$  432.21  $[\text{M} - \text{H}]^-$ , 456.21  $[\text{M} + \text{Na}]^+$ ; LCMS (ESI)  $m/z$  calcd for  $\text{C}_{21}\text{H}_{15}\text{F}_4\text{N}_3\text{O}_3$ : 456.0947  $[\text{M} + \text{Na}]^+$ . Found: 456.0887  $[\text{M} + \text{Na}]^+$ ;  $^1\text{H}$  NMR ( $\text{DMSO}-d_6$ , 400 MHz)  $\delta$  10.35 (bs, 1H,  $\text{NH}$ ), 9.90 (bs, 1H,  $\text{CHO}$ ), 8.25 (s, 1H), 8.24 (d,  $J=2.0$  Hz, 1H), 8.11 (dd,  $J=8.4, 2.0$  Hz, 1H), 8.05 (d,  $J=8.4$  Hz, 1H), 7.70 (dd,  $J=9.0, 2.3$  Hz, 1H), 7.65 (dd,  $J=9.0, 4.4$  Hz, 1H), 7.65 (dt,  $J=9.2, 2.8$  Hz, 1H), 6.51 (s, OH), 4.69 (d,  $J=14.4$  Hz, 1H), 4.42 (d,  $J=14.4$  Hz, 1H), 1.47 (s, 3H);  $^{19}\text{F}$  NMR ( $\text{DMSO}-d_6$ , 400 MHz)  $\delta$  -61.21, -1201.26.

**(S)-N-(6-Cyano-5-(trifluoromethyl)pyridin-3-yl)-3-(5-fluoro-3-formyl-1H-indol-1-yl)-2-hydroxy-2-methylpropanamide (31m).**—Synthetic Method A was used to

produce compound **31m** as a yellowish solid (yield 73%; purity 99.14%). The structure of the product was determined using 2D NMR (COSY and NOESY). MS (ESI)  $m/z$  457.16  $[\text{M} + \text{Na}]^+$ , 433.17  $[\text{M} - \text{H}]^-$ ; LCMS (ESI)  $m/z$  calcd for  $\text{C}_{20}\text{H}_{14}\text{F}_4\text{N}_4\text{O}_3$ : 435.3517  $[\text{M} + \text{H}]^+$ . Found: 434.1113  $[\text{M} + \text{H}]^+$ ;  $^1\text{H}$  NMR (Acetone- $d_6$ , 400 MHz)  $\delta$  10.08 (bs, 1H,  $\text{NH}$ ), 9.95 (bs, 1H,  $\text{CHO}$ ), 9.14 (s, 1H), 8.69 (s, 1H), 7.80 (dd,  $J=9.4, 2.4$  Hz, 1H), 7.66 (dd,  $J=9.2, 4.4$  Hz, 1H), 7.05 (dt,  $J=9.2, 2.4$  Hz, 1H), 5.85 (s, OH), 4.86 (d,  $J=14.8$  Hz, 1H), 4.55 (d,  $J=14.8$  Hz, 1H), 1.68 (s, 3H);  $^{19}\text{F}$  NMR (Acetone- $d_6$ , 400 MHz)  $\delta$  114.53, 54.70.

**(S,Z)-N-(4-Cyano-3-(trifluoromethyl)phenyl)-3-(5-fluoro-3-(hydroxyimino)methyl)-1H-indol-1-yl)-2-hydroxy-2-methylpropanamide**

**(31n).**—Synthetic Method D<sup>37</sup> was used to produce compound **31n** as a pink solid (yield 94%). The structure of the product was determined using 2D NMR (COSY and NOESY). MS (ESI)  $m/z$  447.21 [M – H]<sup>–</sup>; 449.24 [M + H]<sup>+</sup>; 471.23 [M + Na]<sup>+</sup>; HRMS (ESI)  $m/z$  calcd for C<sub>21</sub>H<sub>16</sub>F<sub>4</sub>N<sub>4</sub>O<sub>4</sub>: 449.1237 [M – H]<sup>–</sup>. Found 449.1235 [M – H]<sup>–</sup>; <sup>1</sup>H NMR (DMSO-*d*<sub>6</sub>, 400 MHz)  $\delta$  11.24 (bs, 1H, *NH*), 10.34 (bs, 1H, *OH*), 8.34 (s, 1H), 8.24 (s, 1H), 8.10 (d, *J* = 8.6 Hz, 1H), 8.02 (d, *J* = 8.6 Hz, 1H), 7.73 (s, 1H), 7.65 (dd, *J* = 10.0, 2.4 Hz, 1H), 7.55 (dd, *J* = 9.2, 4.4 Hz, 1H), 6.97 (dt, *J* = 9.2, 2.4 Hz, 1H), 6.46 (s, *OH*), 4.60 (d, *J* = 14.8 Hz, 1H), 4.35 (d, *J* = 14.8 Hz, 1H), 1.43 (s, 3H); <sup>19</sup>F NMR (DMSO-*d*<sub>6</sub>, 400 MHz)  $\delta$  –61.17, –123.69.

**(S)-N-(6-Cyano-5-(trifluoromethyl)pyridin-3-yl)-3-(5-fluoro-3-(hydroxyimino)methyl)-1H-indol-1-yl)-2-hydroxy-2-methylpropanamide**

**(31o).**—Synthetic Method D was used to produce compound **31o** as a brownish solid (yield 43%; purity 99.33%). The structure of the product was determined using 2D NMR (COSY and NOESY). UV max 195.45, 266.45; MS (ESI)  $m/z$  448.19 [M – H]<sup>–</sup>, 450.22 [M + H]<sup>+</sup>; LCMS (ESI)  $m/z$  calcd for C<sub>20</sub>H<sub>15</sub>F<sub>4</sub>N<sub>5</sub>O<sub>3</sub>: 450.1189 [M + H]<sup>+</sup>. Found: 450.1192 [M + H]<sup>+</sup>; <sup>1</sup>H NMR (CDCl<sub>3</sub>, 400 MHz)  $\delta$  9.73 (bs, 1H, *NH*), 9.15 (bs, 1H, *OH*), 8.87 (d, *J* = 2.8 Hz, 1H), 8.80 (d, *J* = 2.0 Hz, 1H), 8.64 (d, *J* = 2.0 Hz, 1H), 7.71 (s, 1H), 7.34–7.28 (m, 2H), 7.02 (dt, *J* = 8.6 Hz, 1H), 8.02 (d, *J* = 8.6 Hz, 1H), 7.73 (s, 1H), 7.65 (dd, *J* = 10.0, 2.4 Hz, 1H), 7.55 (dd, *J* = 9.2, 4.4 Hz, 1H), 6.97 (dt, *J* = 8.8, 2.4 Hz, 1H), 6.46 (s, *OH*), 4.53 (d, *J* = 13.2 Hz, 1H), 4.35 (d, *J* = 13.2 Hz, 1H), 1.57 (s, 3H); <sup>19</sup>F NMR (CDCl<sub>3</sub>, 400 MHz)  $\delta$  –62.18, –121.67.

**(S,E)-3-(3-((2-Acetylhydrazono)methyl)-5-fluoro-1H-indol-1-yl)-N-(4-cyano-3-(trifluoromethyl)phenyl)-2-hydroxy-2-methylpropanamide (31p).**—Synthetic

Method D was used to produce compound **31p** as a yellowish solid *trans/cis* isomer (yield 90.5%). The structure of the product was determined using 2D NMR (COSY and NOESY). HPLC (45% acetonitrile): *t*<sub>R</sub> 3.22 min, purity = 99.33%. MS (ESI)  $m/z$  488.26 [M – H]<sup>–</sup>; 490.28 [M + H]<sup>+</sup>, 512.23 [M + Na]<sup>+</sup>; HRMS (ESI)  $m/z$  calcd for C<sub>23</sub>H<sub>19</sub>F<sub>4</sub>N<sub>5</sub>O<sub>3</sub>: 490.1502 [M + H]<sup>+</sup>, 512.1322 [M + Na]<sup>+</sup>. Found: 490.1509 [M + H]<sup>+</sup>, 512.1328 [M + Na]<sup>+</sup>; <sup>1</sup>H NMR (CDCl<sub>3</sub>, 400 MHz)  $\delta$  9.50 (s, 0.25-H for *cis* type), 9.03 (s, 0.75-H, for *trans* type), 8.97 (s, 0.25-H for *cis* type), 8.61 (s, 0.75-H, for *trans* type), 8.16 (bs, 1H, *NHC(O)* –), 7.83 (m, 1H, *ArH*), 7.72 (s, 2H, *ArH*), 7.54 (m, 1H, *ArH*), 7.52 (s, 1H, *ArH*), 7.42 (dd, *J* = 9.2, 4.2 Hz, 1H, *ArH*), 7.01 (m, 1H, –C=N–*NH*–), 5.96 (s, 0.25-*OH*, for *cis* type), 4.64 (s, 0.75-*OH*, for *trans* type), 4.62 (d, *J* = 14.8 Hz, 0.75-H, for *trans* type), 4.59 (d, *J* = 14.4 Hz, 0.25-H, for *cis* type), 4.42 (d, *J* = 14.4 Hz, 0.25-H, for *cis* type), 4.37 (d, *J* = 14.8 Hz, 0.75H, for *trans* type), 2.30 (s, 3H), 1.66 (s, 3H); <sup>19</sup>F NMR (CDCl<sub>3</sub>, 400 MHz)  $\delta$  –62.22, –121.58.

**(S)-N-(4-Cyano-3-(trifluoromethyl)phenyl)-3-(3-cyano-5-fluoro-1H-indol-1-yl)-2-hydroxy-2-methylpropanamide (31q).**—Synthetic Method A was used to produce

compound **31q** as a brownish solid (yield 63%; purity 98.41%). The structure of the product was determined using 2D NMR (COSY and NOESY). UV  $\lambda_{\max}$  196.45, 270.45 nm; MS (ESI)  $m/z$  429.12 [M – H]<sup>–</sup>, 453.19 [M + Na]<sup>+</sup>; LCMS (ESI)  $m/z$  calcd for C<sub>21</sub>H<sub>14</sub>F<sub>4</sub>N<sub>4</sub>O<sub>2</sub>: 431.1131 [M + H]<sup>+</sup>, 453.0951 [M + Na]<sup>+</sup>. Found: 431.1112 [M + H]<sup>+</sup>, 453.1145 [M + Na]<sup>+</sup>; <sup>1</sup>H NMR (DMSO-*d*<sub>6</sub>, 400 MHz)  $\delta$  10.32 (bs, 1H, *NH*),

8.20 (d,  $J=1.6$  Hz, 1H), 8.19 (s, 1H), 8.07 (dd,  $J=8.6, 1.6$  Hz, 1H), 8.02 (d,  $J=8.6$  Hz, 1H), 7.67 (dd,  $J=9.2, 4.4$  Hz, 1H), 7.33 (dd,  $J=9.2, 2.4$  Hz, 1H), 7.08 (dt,  $J=9.2, 2.4$  Hz, 1H), 6.51 (bs, OH), 4.67 (d,  $J=14.4$  Hz, 1H), 4.37 (d,  $J=14.4$  Hz, 1H), 1.43 (s, 3H);  $^{19}\text{F}$  NMR (DMSO- $d_6$ , 400 MHz)  $\delta$  -61.23, -121.31.

**(S)-N-(6-Cyano-5-(trifluoromethyl) pyridin-3-yl)-3-(3-cyano-5-fluoro-1H-indol-1-yl)-2-hydroxy-2-methylpropanamide (31r).**—Synthetic Method A was used to produce compound **31r** as a yellowish solid (yield 37%; purity 98.78%). The structure of the product was determined using 2D NMR (COSY and NOESY). MS (ESI)  $m/z$  430.21 [M - H]<sup>-</sup>, 432.22 [M + H]<sup>+</sup>; LCMS (ESI)  $m/z$  calcd for C<sub>20</sub>H<sub>13</sub>F<sub>4</sub>N<sub>5</sub>O<sub>2</sub> 432.1084 [M + H]<sup>+</sup>. Found: 432.1055 [M + H]<sup>+</sup>; 454.0878 [M + Na]<sup>+</sup>;  $^1\text{H}$  NMR (DMSO- $d_6$ , 400 MHz)  $\delta$  10.54 (bs, 1H,  $NH$ ), 9.14 (d,  $J=2.0$  Hz, 1H), 8.52 (d,  $J=2.0$  Hz, 1H), 8.20 (s, 1H), 7.65 (dd,  $J=9.2, 4.4$  Hz, 1H), 7.33 (dd,  $J=9.2, 2.4$  Hz, 1H), 7.08 (dt,  $J=9.2, 2.4$  Hz, 1H), 6.58 (bs, OH), 4.69 (d,  $J=14.4$  Hz, 1H), 4.38 (d,  $J=14.4$  Hz, 1H), 1.45 (s, 3H);  $^{19}\text{F}$  NMR (DMSO- $d_6$ , 400 MHz)  $\delta$  -61.38, -121.27.

**(S)-N-(4-Cyano-3-(trifluoromethyl)phenyl)-3-(5-fluoro-3-nitro-1H-indol-1-yl)-2-hydroxy-2-methylpropanamide (31s).**—Synthetic Method A was used to produce compound **31s** as a yellowish solid (yield 42%). The structure of the product was determined using 2D NMR (COSY and NOESY). MS (ESI)  $m/z$  449.20 [M - H]<sup>-</sup>, 451.21 [M + H]<sup>+</sup>; LCMS (ESI)  $m/z$  calcd for C<sub>20</sub>H<sub>14</sub>F<sub>4</sub>N<sub>4</sub>O<sub>4</sub> 451.1029 [M + H]<sup>+</sup>. Found: 451.1026 [M + H]<sup>+</sup>;  $^1\text{H}$  NMR (Acetone- $d_6$ , 400 MHz)  $\delta$  9.88 (bs, 1H,  $NH$ ), 8.47 (s, 1H), 8.22 (d,  $J=2.0$  Hz, 1H), 8.10 (dd,  $J=8.6, 2.0$  Hz, 1H), 7.95 (d,  $J=8.6$  Hz, 1H), 7.74 (dd,  $J=9.2, 3.2$  Hz, 1H), 7.11 (dt,  $J=9.2, 2.4$  Hz, 1H), 5.83 (bs, OH), 4.93 (d,  $J=14.4$  Hz, 1H), 4.56 (d,  $J=14.4$  Hz, 1H), 1.67 (s, 3H);  $^{19}\text{F}$  NMR (Acetone- $d_6$ , 400 MHz)  $\delta$  -62.98, -122.77.

**(S)-N-(4-Cyano-3-(trifluoromethyl)phenyl)-3-(4-fluoro-1H-indazol-1-yl)-2-hydroxy-2-methylpropanamide (32a).**—Synthetic Method C was used to produce compound **32a** (and compound **32b**, see below; total yield of compounds **32a** and **32b**, 65%; yield of compound **32a**, 36% at  $R_f = 0.14$ ). HRMS (ESI)  $m/z$  calcd for C<sub>19</sub>H<sub>15</sub>F<sub>4</sub>N<sub>4</sub>O<sub>2</sub>: 407.1131. Found: 407.1150 [M + H]<sup>+</sup>;  $^1\text{H}$  NMR (CDCl<sub>3</sub>, 400 MHz)  $\delta$  9.10 (bs, 1H,  $NH$ ), 8.11 (d,  $J=0.8$  Hz, 1H), 7.91 (d,  $J=2.0$  Hz, 1H), 7.76 (dd,  $J=8.4, 2.0$  Hz, 1H), 7.71 (d,  $J=8.4$  Hz, 1H), 7.41–7.36 (m, 1H), 7.30 (d,  $J=8.4$  Hz, 1H), 6.80 (dd,  $J=9.6, 7.2$  Hz, 1H), 6.02 (s, 1H, OH), 4.93 (d,  $J=14.0$  Hz, 1H), 4.43 (d,  $J=14.0$  Hz, 1H), 1.53 (s, 3H);  $^{19}\text{F}$  NMR (CDCl<sub>3</sub>, 400 MHz)  $\delta$  -62.25, -117.48.

**(S)-N-(4-Cyano-3-(trifluoromethyl)phenyl)-3-(4-fluoro-2H-indazol-2-yl)-2-hydroxy-2-methylpropanamide (32b).**—Synthetic Method C was used to produce compound **32b** (and compound **32a**, see above; total yield of compounds **32a** and **32b**, 65%; yield of compound **32b**, 29% at  $R_f = 0.12$ ). HRMS (ESI)  $m/z$  calcd for C<sub>19</sub>H<sub>15</sub>F<sub>4</sub>N<sub>4</sub>O<sub>2</sub>: 407.1131. Found: 407.1168 [M + H]<sup>+</sup>;  $^1\text{H}$  NMR (CDCl<sub>3</sub>, 400 MHz)  $\delta$  9.15 (bs, 1H,  $NH$ ), 8.08 (s, 1H), 7.96 (d,  $J=1.6$  Hz, 1H), 7.84 (dd,  $J=8.8, 1.6$  Hz, 1H), 7.74 (d,  $J=8.8$  Hz, 1H), 7.42 (d,  $J=8.8$  Hz, 1H), 7.26 (m, 1H), 6.72 (dd,  $J=10.0, 7.2$  Hz, 1H), 6.67 (bs, 1H, OH), 4.96 (d,  $J=13.6$  Hz, 1H), 4.54 (d,  $J=13.6$  Hz, 1H), 1.54 (s, 3H);  $^{19}\text{F}$  NMR (CDCl<sub>3</sub>, 400 MHz)  $\delta$  -62.41, -116.55.



**(S)-N-(4-Cyano-3-(trifluoromethyl)phenyl)-2-hydroxy-2-methyl-3-(4-(trifluoromethyl)-1H-indazol-1-yl) propenamide (32c).**—Synthetic

Method A was used to produce compound **32c** (yield 28.2%). HRMS

(ESI)  $m/z$  calcd for  $C_{20}H_{14}F_6N_4O_2$  Exact Mass: 457.1099  $[M + H]^+$ . Found: 457.1117  $[M + H]^+$ ;  $^1H$  NMR ( $CDCl_3$ , 400 MHz)  $\delta$  9.08 (bs, 1H, NH), 8.19 (t,  $J = 1.2$  Hz, 1H), 7.90 (d,  $J = 1.6$  Hz, 1H), 7.61–7.70 (m, 3H), 7.55–7.47 (m, 2H), 5.93 (bs, 1H, OH), 5.01 (d,  $J = 14.0$  Hz, 1H), 4.47 (d,  $J = 14.0$  Hz, 1H), 1.55 (s, 3H);  $^{19}F$  NMR ( $CDCl_3$ , 400 MHz)  $\delta$  –61.54, 62.27.

**(S)-N-(4-Cyano-3-(trifluoromethyl)phenyl)-2-hydroxy-2-methyl-3-(4-(trifluoromethyl)-2H-indazol-2-yl) propenamide (32d).**—Synthetic

Method A was used to produce compound

**32d** (yield 30.1%). HRMS (ESI)  $m/z$  calcd for  $C_{20}H_{14}F_6N_4O_2$  Exact Mass 457.1099  $[M + H]^+$ . Found: 457.1110  $[M + H]^+$ ;  $^1H$  NMR ( $CDCl_3$ , 400 MHz)  $\delta$  9.09 (bs, 1H, NH), 8.14 (s, 1H), 7.92 (d,  $J = 2.0$  Hz, 1H), 7.85–7.82 (m, 1H), 7.73 (d,  $J = 8.4$  Hz, 1H), 7.44 (dt,  $J = 6.8, 0.8$  Hz, 1H), 7.41 (q,  $J = 8.4$  Hz, 1H), 6.56 (bs, 1H, OH), 4.98 (d,  $J = 14.0$  Hz, 1H), 4.57 (d,  $J = 14.0$  Hz, 1H), 1.54 (s, 3H);  $^{19}F$  NMR ( $CDCl_3$ , 400 MHz)  $\delta$  –61.28, 62.55.

**(S)-N-(4-Cyano-3-(trifluoromethyl)phenyl)-3-(5-fluoro-2H-benzo[d][1,2,3]triazol-2-yl)-2-hydroxy-2-methylpropanamide (34a).**—Synthetic

Method A was used to produce compound **34a** as a yellowish solid (yield

19.4%). Mass (ESI)  $m/z$  430.09  $[M + Na]^+$ ;  $^1H$  NMR (400 MHz, DMSO- $d_6$ )  $\delta$  10.35 (s, 1H, NH), 8.43 (s, 1H, ArH), 8.32 (d,  $J = 8.2$  Hz, 1H, ArH), 8.11 (d,  $J = 8.2$  Hz, 1H, ArH), 7.95–7.91 (m, 1H, ArH), 7.67 (d,  $J = 8.8$  Hz, 1H, ArH), 7.33–6–7.31 (m, 1H, ArH), 6.53 (s, 1H, OH), 5.14 (d,  $J = 13.6$  Hz, 1H, CH), 4.90 (d,  $J = 13.6$  Hz, 1H, CH), 1.53 (s, 3H,  $CH_3$ ).

**(S)-N-(4-Cyano-3-(trifluoromethyl)phenyl)-3-(5-fluoro-1H-benzo[d][1,2,3]triazol-1-yl)-2-hydroxy-2-methylpropanamide (34b).**—Synthetic

Method A was used to produce compound **34b** as a yellowish solid (yield

12.6%). Mass (ESI)  $m/z$  430.09  $[M + Na]^+$ ;  $^1H$  NMR (400 MHz, DMSO- $d_6$ )  $\delta$  10.35 (s, 1H, NH), 8.40 (s, 1H, ArH), 8.19 (d,  $J = 8.4$  Hz, 1H, ArH), 8.10 (d,  $J = 8.0$  Hz, 1H, ArH), 8.07–8.04 (m, 1H, ArH), 7.70 (d,  $J = 8.2$  Hz, 1H, ArH), 7.28–6–7.23 (m, 1H, ArH), 6.45 (s, 1H, OH), 5.05 (d,  $J = 14.4$  Hz, 1H, CH), 4.87 (d,  $J = 14.4$  Hz, 1H, CH), 1.50 (s, 3H,  $CH_3$ ).

**(S)-N-(4-Cyano-3-(trifluoromethyl)phenyl)-3-(6-fluoro-1H-benzo[d][1,2,3]triazol-1-yl)-2-hydroxy-2-methylpropanamide (34c).**—Synthetic

Method A was used to produce compound **34c** as a yellowish solid (yield

8.8%). Mass (ESI)  $m/z$  430.09  $[M + Na]^+$ ;  $^1H$  NMR (400 MHz, DMSO- $d_6$ )  $\delta$  10.35 (s, 1H, NH), 8.38 (s, 1H, ArH), 8.20 (d,  $J = 8.8$  Hz, 1H, ArH), 8.10 (d,  $J = 8.4$  Hz, 1H, ArH), 7.92–7.89 (m, 1H, ArH), 7.84 (d,  $J = 8.8$  Hz, 1H, ArH), 7.46–7.42 (m, 1H, ArH), 6.46 (s, 1H, OH), 5.08 (d,  $J = 14.4$  Hz, 1H, CH), 4.90 (d,  $J = 14.4$  Hz, 1H, CH), 1.49 (s, 3H,  $CH_3$ ).

**(S)-N-(4-Cyano-3-(trifluoromethyl)phenyl)-2-hydroxy-2-methyl-3-(5-(trifluoromethyl)-2H-benzo[d][1,2,3] triazol-2-yl)propenamide (34d).**

—Synthetic Method A was used to produce compound **34d** as

a yellowish solid (yield 9%). Mass (ESI)  $m/z$  456.25  $[M - H]^-$ ; 458.10  $[M + H]^+$ ;  $^1H$  NMR

(400 MHz, DMSO- $d_6$ )  $\delta$  10.33 (s, 1H, NH), 8.40 (s, 1H, ArH), 8.38 (s, 1H, ArH), 8.23 (d,  $J$  = 8.4 Hz, 1H, ArH), 8.11 (d,  $J$  = 8.4 Hz, 2H, ArH), 7.67 (d,  $J$  = 8.6 Hz, 1H, ArH), 6.67 (s, 1H, OH), 5.24 (d,  $J$  = 14.0 Hz, 1H, CH), 4.99 (d,  $J$  = 14.0 Hz, 1H, CH), 1.55 (s, 3H, CH<sub>3</sub>).

**(S)-N-(4-Cyano-3-(trifluoromethyl)phenyl)-2-hydroxy-2-methyl-3-(5-(trifluoromethyl)-1H-benzo[d][1,2,3] triazol-1-yl)propenamide (34e).**

—Synthetic Method A was used to produce

compound **34e** as a yellowish solid (yield 5%). Mass (ESI)  $m/z$  456.25

[M – H]<sup>–</sup>; 458.10 [M + H]<sup>+</sup>; <sup>1</sup>H NMR (400 MHz, DMSO- $d_6$ )  $\delta$  10.30 (s, 1H, NH), 8.39 (d,  $J$  = 1.6 Hz, 1H, ArH), 8.33 (s, 1H, ArH), 8.25 (d,  $J$  = 8.8 Hz, 1H, ArH), 8.12 (dd,  $J$  = 8.8, 2.0 Hz, 1H, ArH), 8.07 (d,  $J$  = 8.4 Hz, 1H, ArH), 7.64 (dd,  $J$  = 8.8, 1.6 Hz, 1H, ArH), 6.64 (s, 1H, OH), 5.21 (d,  $J$  = 14.4 Hz, 1H, CH), 5.01 (d,  $J$  = 14.4 Hz, 1H, CH), 1.54 (s, 3H, CH<sub>3</sub>).

**(S)-N-(4-Cyano-3-(trifluoromethyl)phenyl)-2-hydroxy-2-methyl-3-(6-(trifluoromethyl)-1H-benzo[d][1,2,3] triazol-1-yl)propenamide (34f).**

—Synthetic Method A was used to produce

compound **34f** as a yellowish solid (yield 5%). Mass (ESI)  $m/z$  456.25

[M – H]<sup>–</sup>; 458.10 [M + H]<sup>+</sup>; <sup>1</sup>H NMR (400 MHz, DMSO- $d_6$ )  $\delta$  10.31 (s, 1H, NH), 8.50 (s, 1H, ArH), 8.34 (d,  $J$  = 1.6 Hz, 1H, ArH), 8.18 (dd,  $J$  = 8.8, 2.0 Hz, 1H, ArH), 8.10 (d,  $J$  = 8.8 Hz, 1H, ArH), 8.08 (d,  $J$  = 8.4 Hz, 1H, ArH), 7.84 (dd,  $J$  = 8.8, 1.6 Hz, 1H, ArH), 6.49 (s, 1H, OH), 5.15 (d,  $J$  = 14.4 Hz, 1H, CH), 4.97 (d,  $J$  = 14.4 Hz, 1H, CH), 1.52 (s, 3H, CH<sub>3</sub>).

**(S)-3-(5-Bromo-1H-benzo[d][1,2,3]triazol-1-yl)-N-(4-cyano-3-(trifluoromethyl)phenyl)-2-hydroxy-2-methylpropanamide (34g).**—Synthetic

Method A was used to produce compound **34g** (yield

58%). MS (ESI)  $m/z$  467.81 [M – H]<sup>–</sup>; 492.00 [M + Na]<sup>+</sup>; <sup>1</sup>H NMR (400 MHz, CDCl<sub>3</sub>)  $\delta$  9.10 (bs, 1H, NH), 8.04 (s, 1H), 8.02 (s, 1H), 7.90 (d,  $J$  = 8.0 Hz, 1H), 7.76 (d,  $J$  = 8.0 Hz, 1H), 7.74 (d,  $J$  = 8.8 Hz, 1H), 7.49 (d,  $J$  = 8.8 Hz, 1H), 5.48 (s, 1H, OH), 5.26 (d,  $J$  = 13.6 Hz, 1H), 4.94 (d,  $J$  = 13.6 Hz, 1H), 1.54 (s, 3H); <sup>19</sup>F NMR (CDCl<sub>3</sub>, decoupled)  $\delta$  –62.19.

**(S)-N-(4-Cyano-3-(trifluoromethyl) phenyl)-3-(5-(4-fluorophenyl)-1H-benzo[d][1,2,3] triazol-1-yl)-2-hydroxy-2-methylpropanamide (34h).**—A mixture of

compound **34g** (150 mg, 0.32 mmol), tetrakis(triphenylphosphine)palladium(0) (13 mg, 12 mmol), and trimethoxy boric acid (50 mg, 0.35 mmol) in THF/MeOH (1/1 mL) with sodium carbonate (82 mg, 7.69 mmol) in ethanol/H<sub>2</sub>O (5 mL/1 mL) were heated to reflux overnight. The mixture was cooled to be concentrated under reduced pressure, poured into EtOAc, washed with H<sub>2</sub>O, dried over MgSO<sub>4</sub>, concentrated, and purified by silica gel chromatography (EtOAc:*n*-hexane 2:3) to produce compound **34h** as a yellow solid (yield 90%). MS (ESI)  $m/z$  482.25 [M – H]<sup>–</sup>; <sup>1</sup>H NMR (400 MHz, CDCl<sub>3</sub>)  $\delta$  9.12 (bs, 1H, NH), 8.02 (s, 1H), 7.96 (s, 1H), 7.92 (d,  $J$  = 9.2 Hz, 1H), 7.76 (d,  $J$  = 8.4 Hz, 1H), 7.64 (d,  $J$  = 9.2 Hz, 1H), 7.59 (dd,  $J$  = 7.6, 5.2 Hz, 2H), 7.17 (t,  $J$  = 8.4 Hz, 2H), 5.72 (s, 1H, OH), 5.28 (d,  $J$  = 14.0 Hz, 1H), 4.97 (d,  $J$  = 14.0 Hz, 1H), 1.55 (s, 3H); <sup>19</sup>F NMR (CDCl<sub>3</sub>, decoupled)  $\delta$  –62.20, –114.49.

**(S)-N-(4-Cyano-3-(trifluoromethyl)phenyl)-3-(3,5-difluoro-1H-indazol-1-yl)-2-hydroxy-2-methylpropanamide (35a).**

—Synthetic Method A was used to produce compound **35a** as a white solid (yield 57%). MS (ESI)  $m/z$  423.17 [M – H]<sup>–</sup>; 447.21 [M + Na]<sup>+</sup>; <sup>1</sup>H NMR (CDCl<sub>3</sub>, 400 MHz)  $\delta$  9.07 (bs, 1H, *NH*), 7.92 (s, 1H), 7.78 (d,  $J$  = 8.6 Hz, 1H), 7.73 (d,  $J$  = 8.6 Hz, 1H), 7.42 (d,  $J$  = 8.4 Hz, 1H), 7.28 (m, 1H), 7.25 (m, 1H), 5.28 (bs, 1H, OH), 4.82 (d,  $J$  = 14.0 Hz, 1H), 4.27 (d,  $J$  = 14.0 Hz, 1H), 1.52 (s, 3H); <sup>19</sup>F NMR (CDCl<sub>3</sub>, 400 MHz)  $\delta$  –61.27, –120.39, –131.15.

**(S)-N-(6-Cyano-5-(trifluoromethyl)pyridin-3-yl)-3-(3,5-difluoro-1H-indazol-1-yl)-2-hydroxy-2-methylpropanamide (35b).**

—Synthetic Method A was used to produce compound **35b** (yield 56%). MS (ESI)  $m/z$  424.18 [M – H]<sup>–</sup>; 426.22 [M + H]<sup>+</sup>; HRMS (ESI)  $m/z$  calcd for C<sub>18</sub>H<sub>12</sub>F<sub>5</sub>N<sub>5</sub>O<sub>2</sub>: 426.0989 [M + H]<sup>+</sup>. Found: 426.0997 [M + H]<sup>+</sup>; <sup>1</sup>H NMR (CDCl<sub>3</sub>, 400 MHz)  $\delta$  9.20 (bs, 1H, *NH*), 8.79 (s, 1H), 8.55 (s, 1H), 7.41 (s, 1H), 7.26 (m, 2H), 5.41 (bs, 1H, OH), 4.82 (d,  $J$  = 12.4 Hz, 1H), 4.29 (d,  $J$  = 12.4 Hz, 1H), 1.54 (s, 3H); <sup>19</sup>F NMR (CDCl<sub>3</sub>, 400 MHz)  $\delta$  –85.46, –156.21, –175.96.

**(S)-3-(3-Chloro-5-fluoro-1H-indazol-1-yl)-N-(4-cyano-3-(trifluoromethyl)phenyl)-2-hydroxy-2-methylpropanamide (35c).**

—Synthetic Method A was used to produce compound **35c** as a brownish solid (yield 58%; purity 94.93%; MP 172.5–173.6 °C). The structure of the product was determined using 2D NMR (COSY and NOESY). MS (ESI)  $m/z$  439.20 [M – H]<sup>–</sup>, LCMS (ESI)  $m/z$  calcd for C<sub>19</sub>H<sub>13</sub>ClF<sub>4</sub>N<sub>4</sub>O<sub>2</sub> 441.0741 [M + H]<sup>+</sup>. Found: 441.0703 [M + H]<sup>+</sup>; <sup>1</sup>H NMR (Acetone-*d*<sub>6</sub>, 400 MHz)  $\delta$  9.83 (bs, 1H, *NH*), 8.36 (d,  $J$  = 2.0 Hz, 1H), 8.18 (dd,  $J$  = 8.8, 2.0 Hz, 1H), 8.00 (d,  $J$  = 8.8 Hz, 1H), 7.77 (dd,  $J$  = 10.0, 4.0 Hz, 1H), 7.32–7.28 (m, 2H), 5.44 (bs, OH), 4.90 (d,  $J$  = 14.8 Hz, 1H), 4.62 (d,  $J$  = 14.8 Hz, 1H), 1.61 (s, 3H); <sup>19</sup>F NMR (Acetone-*d*<sub>6</sub>, 400 MHz)  $\delta$  –62.82, –122.89.

**(S)-3-(3-Chloro-5-fluoro-1H-indazol-1-yl)-N-(6-cyano-5-(trifluoromethyl)pyridin-3-yl)-2-hydroxy-2-methylpropanamide (35d).**

—Synthetic Method A was used to produce compound **35d** as a white solid (yield 88%; purity 97.54%). The structure of the product was determined using 2D NMR (COSY and NOESY). MS (ESI)  $m/z$  440.09 [M – H]<sup>–</sup>, 442.41 [M + H]<sup>+</sup>; LCMS (ESI)  $m/z$  calcd for C<sub>18</sub>H<sub>12</sub>ClF<sub>4</sub>N<sub>5</sub>O<sub>2</sub>: 442.0694 [M + H]<sup>+</sup>, 464.0513 [M + Na]<sup>+</sup>. Found: 442.0652 [M + H]<sup>+</sup>, 464.0510 [M + Na]<sup>+</sup>; <sup>1</sup>H NMR (Acetone-*d*<sub>6</sub>, 400 MHz)  $\delta$  10.03 (bs, 1H, *NH*), 9.19 (d,  $J$  = 1.8 Hz, 1H), 8.80 (d,  $J$  = 1.8 Hz, 1H), 7.76 (m, 1H), 7.73–2.30 (m, 2H), 5.53 (bs, OH), 4.89 (d,  $J$  = 14.8 Hz, 1H), 4.65 (d,  $J$  = 14.8 Hz, 1H), 1.63 (s, 3H); <sup>19</sup>F NMR (Acetone-*d*<sub>6</sub>, 400 MHz)  $\delta$  –62.93, –122.86.

**(S)-3-(3-Bromo-5-fluoro-1H-indazol-1-yl)-N-(6-cyano-5-(trifluoromethyl)pyridin-3-yl)-2-hydroxy-2-methylpropanamide (35e).**

—Synthetic Method A was used to produce compound **35e** as a white solid (yield 58%). The structure of the product was determined using 2D NMR (COSY and NOESY). MS (ESI)  $m/z$  485.07 [M – H]<sup>–</sup>, 487.11 [M + H]<sup>+</sup>; 508.12 [M + Na]<sup>+</sup>; LCMS (ESI)  $m/z$  calcd for C<sub>18</sub>H<sub>12</sub>BrF<sub>4</sub>N<sub>5</sub>O<sub>2</sub> 486.0189 [M + H]<sup>+</sup> found 486.0187 [M + H]<sup>+</sup>; 484.0032; <sup>1</sup>H NMR (CDCl<sub>3</sub>, 400 MHz)  $\delta$  9.24 (bs, 1H, *NH*), 8.79 (d,  $J$  = 2.0 Hz, 1H), 8.54 (d,  $J$  = 2.0 Hz, 1H), 7.49 (dd,  $J$  = 8.0, 2.0

Hz, 1H), 7.31–7.27 (m, 1H), 7.26–7.21 (m, 1H), 5.63 (bs, OH), 4.93 (d,  $J = 14.4$  Hz, 1H), 4.42 (d,  $J = 14.4$  Hz, 1H), 1.58 (s, 3H);  $^{19}\text{F}$  NMR ( $\text{CDCl}_3$ , 400 MHz)  $\delta -62.17, -119.40$ .

**(S)-N-(6-Cyano-5-(trifluoromethyl)pyridin-3-yl)-3-(5-fluoro-3-iodo-1H-indazol-1-yl)-2-hydroxy-2-methylpropanamide (35f).**—Synthetic Method A was used to produce compound **35f** as a white solid (yield 63%; purity 98.95%). The structure of the product was determined using 2D NMR (COSY and NOESY). MS (ESI)  $m/z$  532.03  $[\text{M} - \text{H}]^-$ , 556.04  $[\text{M} + \text{Na}]^+$ ; LCMS (ESI)  $m/z$  calcd for  $\text{C}_{18}\text{H}_{12}\text{F}_4\text{IN}_5\text{O}_2$  534.0050  $[\text{M} + \text{H}]^+$ . Found: 534.0048  $[\text{M} + \text{H}]^+$ ;  $^1\text{H}$  NMR ( $\text{CDCl}_3$ , 400 MHz)  $\delta$  9.23 (bs, 1H,  $\text{NH}$ ), 8.78 (d,  $J = 2.4$  Hz, 1H), 8.54 (d,  $J = 2.4$  Hz, 1H), 7.47 (dd,  $J = 9.2, 3.6$  Hz, 1H), 7.30 (dt,  $J = 8.8, 2.4$  Hz, 1H), 7.11 (dd,  $J = 8.0, 2.4$  Hz, 1H), 5.56 (bs, OH), 4.95 (d,  $J = 14.0$  Hz, 1H), 4.45 (d,  $J = 14.0$  Hz, 1H), 1.56 (s, 3H);  $^{19}\text{F}$  NMR ( $\text{CDCl}_3$ , 400 MHz)  $\delta -62.17, -119.49$ .

**(S)-N-(6-Cyano-5-(trifluoromethyl)pyridin-3-yl)-3-(5-fluoro-3-methyl-1H-indazol-1-yl)-2-hydroxy-2-methylpropanamide (35g).**—Synthetic Method A was used to produce compound **35g** as a white solid (yield 68%; purity 98.85%; MP 172.5–173.6 °C). The structure of the product was determined using 2D NMR (COSY and NOESY). UV  $\lambda_{\text{max}}$  196.45, 270.45 nm; MS (ESI)  $m/z$  420.20  $[\text{M} - \text{H}]^-$ , 422.32  $[\text{M} + \text{H}]^+$ , 444.26  $[\text{M} + \text{Na}]^+$ ; LCMS (ESI)  $m/z$  calcd for  $\text{C}_{19}\text{H}_{15}\text{F}_4\text{N}_5\text{O}_2$ : 420.1084  $[\text{M} - \text{H}]^-$ . Found: 420.1101  $[\text{M} - \text{H}]^-$ ;  $^1\text{H}$  NMR ( $\text{CDCl}_3$ , 400 MHz)  $\delta$  9.30 (bs, 1H,  $\text{NH}$ ), 8.75 (d,  $J = 2.2$  Hz, 1H), 8.56 (d,  $J = 2.2$  Hz, 1H), 7.39 (dd,  $J = 8.8, 4.0$  Hz, 1H), 7.25–7.19 (m, 2H), 6.38 (bs, OH), 4.85 (d,  $J = 14.0$  Hz, 1H), 4.33 (d,  $J = 14.0$  Hz, 1H), 2.53 (s, 3H), 1.53 (s, 3H);  $^{19}\text{F}$  NMR ( $\text{CDCl}_3$ , 400 MHz)  $\delta -62.18, -122.23$ .

**(S)-3-(3-Chloro-4-(trifluoromethyl)-1H-indazol-1-yl)-N-(4-cyano-3-(trifluoromethyl)phenyl)-2-hydroxy-2-methylpropanamide (35h).**—Synthetic Method A was used to produce compound **35h** (yield 68%; purity 98.79%; UV max 214.45, 271.45). MS (ESI)  $m/z$  489.20  $[\text{M} - \text{H}]^-$ ; LCMS (ESI)  $m/z$  calcd for  $\text{C}_{20}\text{H}_{13}\text{ClF}_6\text{N}_4\text{O}_2$ : 489.0553  $[\text{M} - \text{H}]^-$ . Found: 489.0582  $[\text{M} - \text{H}]^-$ ; 491.0709  $[\text{M} + \text{H}]^+$  found 491.0713;  $^1\text{H}$  NMR ( $\text{CDCl}_3$ , 400 MHz)  $\delta$  9.08 (bs, 1H,  $\text{NH}$ ), 7.95 (s, 1H), 7.78–7.73 (m, 3H), 7.59–7.55 (m, 2H), 5.31 (bs, OH), 5.00 (d,  $J = 14.2$  Hz, 1H), 4.53 (d,  $J = 14.2$  Hz, 1H), 1.57 (s, 3H).  $^{19}\text{F}$  NMR ( $\text{CDCl}_3$ , 400 MHz)  $\delta -58.26, -62.27$ .

**(S)-3-(3-Chloro-4-(trifluoromethyl)-1H-indazol-1-yl)-N-(6-cyano-5-(trifluoromethyl)pyridin-3-yl)-2-hydroxy-2-methylpropanamide (35i).**—Synthetic Method A was used to produce compound **35i** (yield 48%; purity 99.99%; UV max: 284.45). MS (ESI)  $m/z$  490.06  $[\text{M} - \text{H}]^-$ ; LCMS (ESI)  $m/z$  calcd for  $\text{C}_{19}\text{H}_{12}\text{ClF}_6\text{N}_5\text{O}_2$ : 490.0505  $[\text{M} - \text{H}]^-$ . Found: 490.0509  $[\text{M} - \text{H}]^-$ ;  $^1\text{H}$  NMR ( $\text{CDCl}_3$ , 400 MHz)  $\delta$  9.22 (bs, 1H,  $\text{NH}$ ), 8.81 (d,  $J = 2.2$  Hz, 1H), 8.54 (d,  $J = 2.2$  Hz, 1H), 7.75 (d,  $J = 8.0$  Hz, 1H), 7.58 (m, 2H), 5.42 (bs, OH), 5.01 (d,  $J = 14.4$  Hz, 1H), 4.45 (d,  $J = 14.4$  Hz, 1H), 1.59 (s, 3H);  $^{19}\text{F}$  NMR ( $\text{CDCl}_3$ , 400 MHz)  $\delta -58.22, -62.10$ .

**(S)-N-(6-Cyano-5-(trifluoromethyl)pyridin-3-yl)-3-(5-fluoro-3-formyl-1H-indazol-1-yl)-2-hydroxy-2-methylpropanamide (35j).**—Synthetic Method A was used to produce compound **35j** (yield 28%; purity 98.12%). MS

(ESI)  $m/z$  434.18 [M – H]<sup>–</sup>, 436.29 [M + H]<sup>+</sup>; 458.22 [M + Na]<sup>+</sup>; LCMS (ESI)  $m/z$  calcd for C<sub>19</sub>H<sub>13</sub>F<sub>4</sub>N<sub>5</sub>O<sub>3</sub>: 436.1033 [M + H]<sup>+</sup>. Found: 436.1003 [M + H]<sup>+</sup>; <sup>1</sup>H NMR (CDCl<sub>3</sub>, 400 MHz)  $\delta$  10.27 (s, CHO, 0.4H), 10.20 (s, CHO, 0.6H), 9.16 (bs, 0.6H, NH), 9.13 (bs, 0.4H, NH), 8.79 (d,  $J$  = 2.4 Hz, 0.6H), 8.75 (d,  $J$  = 2.4 Hz, 0.4H), 8.67 (d,  $J$  = 2.4 Hz, 0.4H), 8.55 (d,  $J$  = 2.4 Hz, 0.6H), 7.91 (dd,  $J$  = 8.2, 2.4 Hz, 0.6H), 7.78 (dd,  $J$  = 9.4, 4.8 Hz, 0.4H), 7.63 (dd,  $J$  = 8.2, 2.4 Hz, 0.4H), 7.59 (dd,  $J$  = 9.4, 3.6 Hz, 0.6H), 7.34 (td,  $J$  = 8.8, 2.4 Hz, 0.6H), 7.25 (td,  $J$  = 9.2, 2.4 Hz, 0.4H), 5.75 (bs, 0.4OH), 5.46 (d,  $J$  = 14.4 Hz, 0.4H), 5.33 (bs, 0.6OH), 5.07 (d,  $J$  = 14.4 Hz, 0.6H), 5.03 (d,  $J$  = 14.4 Hz, 0.4H), 4.57 (d,  $J$  = 14.4 Hz, 0.6H), 1.62 (s, 3H). <sup>19</sup>F NMR (CDCl<sub>3</sub>, 400 MHz)  $\delta$  –62.11 (–62.17), –111.05 (–116.25).

**(S)-N-(3-Chloro-4-cyanophenyl)-3-(3-chloro-5-fluoro-1H-indazol-1-yl)-2-hydroxy-2-methylpropanamide (35k).**—Synthetic Method A was

used to produce compound **35k** (yield 67%; purity 97.54%;

UV  $\lambda_{\max}$  269.45 nm). MS (ESI)  $m/z$  405.20 [M – H]<sup>–</sup>, LCMS

(ESI)  $m/z$  calcd for C<sub>18</sub>H<sub>13</sub>Cl<sub>2</sub>FN<sub>4</sub>O<sub>2</sub>: 405.0321 [M – H]<sup>–</sup>. Found: 405.0352 [M – H]<sup>–</sup>; <sup>1</sup>H NMR (CDCl<sub>3</sub>, 400 MHz)  $\delta$  8.96 (bs, 1H, NH), 7.80 (s, 1H), 7.56 (d,  $J$  = 8.4 Hz, 1H), 7.48 (m, 1H), 7.38 (d,  $J$  = 8.4 Hz, 1H), 7.30–7.27 (m, 2H), 5.33 (bs, OH), 4.90 (d,  $J$  = 14.0 Hz, 1H), 4.36 (d,  $J$  = 14.0 Hz, 1H), 1.53 (s, 3H). <sup>19</sup>F NMR (CDCl<sub>3</sub>, 400 MHz)  $\delta$  –119.75.

## Supplementary Material

Refer to Web version on PubMed Central for supplementary material.

## ACKNOWLEDGMENTS

This research was supported by a research grant from National Cancer Institute (NCI) to RN and DDM (1R01CA229164). We thank Covance Laboratories Inc. for metabolism study and Dr. Dejian Ma of UTHSC, College of Pharmacy for assistance with 2D NMR and HRMS experiments. We thank Dr. Kyle Johnson Moore of the UTHSC Office of Scientific Writing for editing the manuscript.

## ABBREVIATIONS USED

<b>2-D</b>	2-Dimensional
<b>ADT</b>	androgen deprivation therapy
<b>AF-1</b>	AR activation functional domain-1
<b>AR</b>	Androgen receptor
<b>AR-V7</b>	AR splice variant 7
<b>CDCl<sub>3</sub></b>	chloroform
<b>COSY</b>	Correlated spectroscopy
<b>CRPC</b>	Castration-resistant prostate cancer
<b>CSFBS</b>	charcoal-stripped FBS
<b>DHT</b>	5 $\alpha$ -Dihydrotestosterone

<b>DMPK</b>	drug metabolism and pharmacokinetics
<b>DMSO</b>	dimethyl sulfoxide
<b>Enz-Res</b>	Enzalutamide resistance
<b>EtOAc</b>	ethyl acetate
<b>EWG</b>	electron withdrawing group
<b>FBS</b>	fetal bovine serum
<b>FL</b>	full-length
<b>GRE</b>	glucocorticoid response element
<b>HIV</b>	human immunodeficiency virus
<b>HRT</b>	Hormone replacement therapy
<b>LBD</b>	Ligand binding domain
<b>LCMS</b>	liquid chromatography/mass spectrometry
<b>MIB</b>	Milbolerone
<b>MLM</b>	mouse liver microsomes
<b>NNRTI</b>	non-nucleoside reverse transcriptase inhibitor
<b>NOE</b>	Nuclear Overhauser effect
<b>NSG mouse</b>	NOD SCID gamma mouse
<b>NMR</b>	nuclear magnetic resonance
<b>NTD</b>	N-terminal domain
<b>PC</b>	Prostate cancer
<b>PROTAC</b>	proteolysis-targeting chimaera
<b>PSA</b>	Prostate-specific antigen
<b>RLU</b>	Relative light units
<b>SAR</b>	Structure–activity relationship
<b>SARD</b>	Selective AR degrader
<b>SARM</b>	selective androgen receptor modulator
<b>SV</b>	Splice variant
<b>T</b>	Testosterone
<b>TGI</b>	tumor growth inhibition



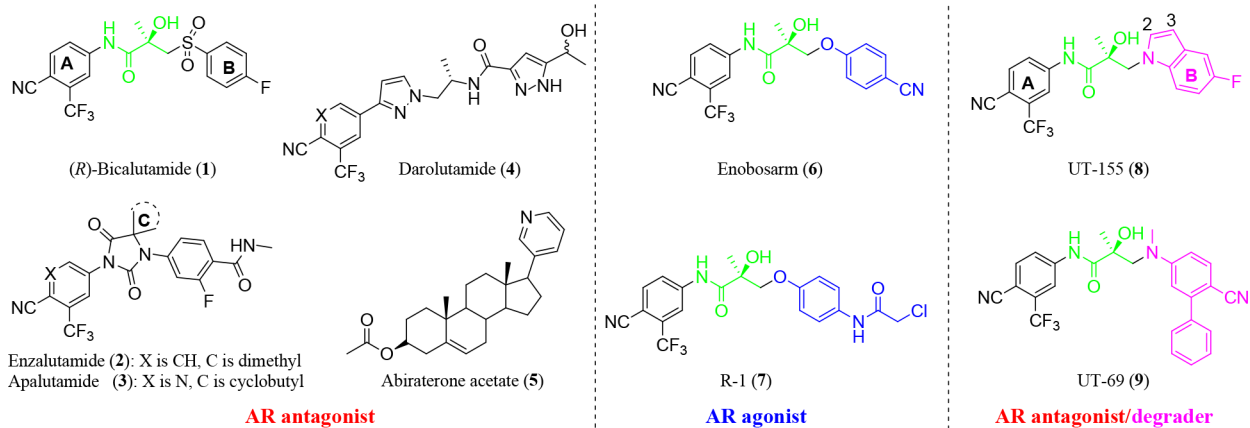
<b>THF</b>	tetrahydrofuran
<b>TLC</b>	thin-layer chromatography
<b>TMS</b>	tetramethylsilane

## REFERENCES

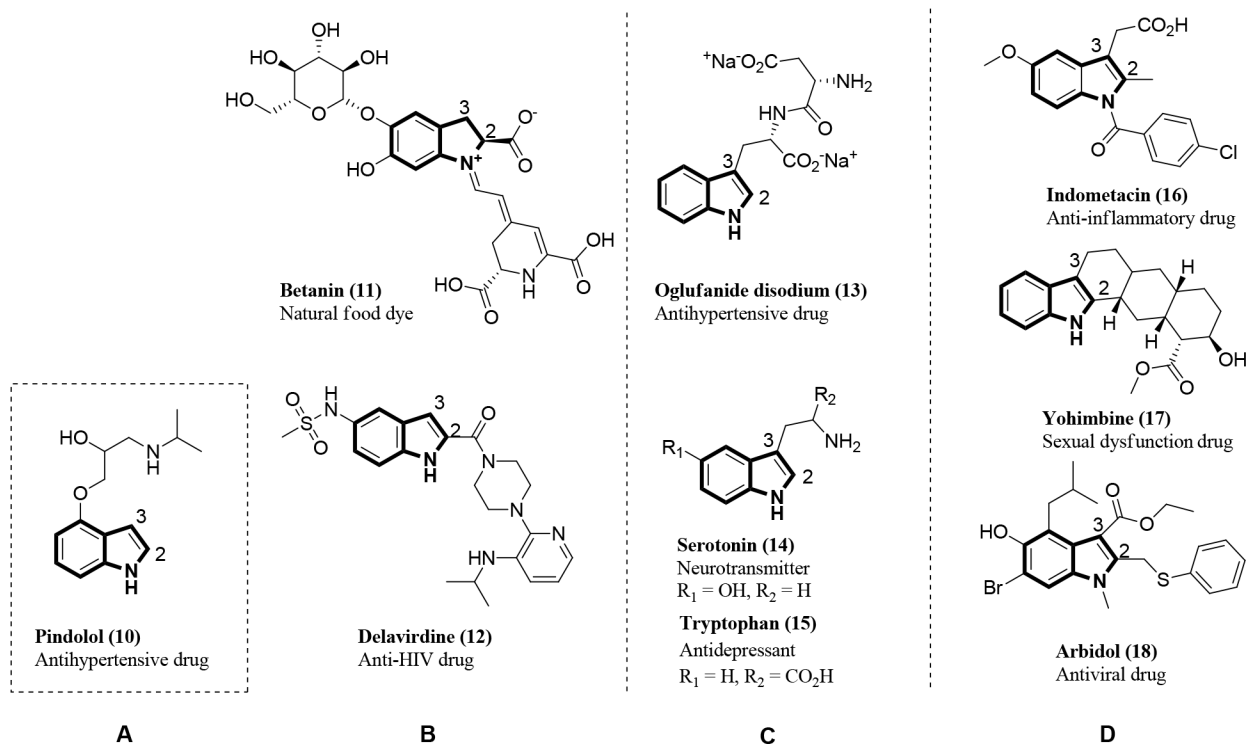
- (1). Estebanez-Perpina E; Bevan CL; McEwan IJ Eighty Years of Targeting Androgen Receptor Activity in Prostate Cancer: The Fight Goes on. *Cancers (Basel)* 2021, 13, 509. [PubMed: 33572755]
- (2). Miller KD; Nogueira L; Mariotto AB; Rowland JH; Yabroff KR; Alfano CM; Jemal A; Kramer JL; Siegel RL Cancer treatment and survivorship statistics, 2019. *CA Cancer J. Clin.* 2019, 69, 363–385. [PubMed: 31184787]
- (3). Taplin ME; Balk SP Androgen receptor: a key molecule in the progression of prostate cancer to hormone independence. *J. Cell Biochem.* 2004, 91, 483–490. [PubMed: 14755679]
- (4). Fujita K; Nonomura N Role of Androgen Receptor in Prostate Cancer: A Review. *World J. Mens Health* 2019, 37, 288–295. [PubMed: 30209899]
- (5). Cockshott ID Bicalutamide: clinical pharmacokinetics and metabolism. *Clin. Pharmacokinet* 2004, 43, 855–878. [PubMed: 15509184]
- (6). Kirkovsky L; Mukherjee A; Yin D; Dalton JT; Miller DD Chiral nonsteroidal affinity ligands for the androgen receptor. 1. Bicalutamide analogues bearing electrophilic groups in the B aromatic ring. *J. Med. Chem.* 2000, 43, 581–590. [PubMed: 10691684]
- (7). Gibbons JA; Ouatas T; Krauwinkel W; Ohtsu Y; van der Walt JS; Beddo V; de Vries M; Mordenti J Clinical Pharmacokinetic Studies of Enzalutamide. *Clin. Pharmacokinet* 2015, 54, 1043–1055. [PubMed: 25917876]
- (8). Rathkopf DE; Morris MJ; Fox JJ; Danila DC; Slovin SF; Hager JH; Rix PJ; Chow Maneval E; Chen I; Gonen M; et al. Phase I study of ARN-509, a novel antiandrogen, in the treatment of castration-resistant prostate cancer. *J. Clin. Oncol.* 2013, 31, 3525–3530. [PubMed: 24002508]
- (9). Fizazi K; Massard C; Bono P; Jones R; Kataja V; James N; Garcia JA; Protheroe A; Tammela TL; Elliott T; et al. Activity and safety of ODM-201 in patients with progressive metastatic castration-resistant prostate cancer (ARADES): an open-label phase I dose-escalation and randomised phase 2 dose expansion trial. *Lancet Oncol.* 2014, 15, 975–985. [PubMed: 24974051]
- (10). Benoist GE; Hendriks RJ; Mulders PF; Gerritsen WR; Somford DM; Schalken JA; van Oort IM; Burger DM; van Erp NP Pharmacokinetic Aspects of the Two Novel Oral Drugs Used for Metastatic Castration-Resistant Prostate Cancer: Abiraterone Acetate and Enzalutamide. *Clin. Pharmacokinet* 2016, 55, 1369–1380. [PubMed: 27106175]
- (11). Hwang DJ; Yang J; Xu H; Rakov IM; Mohler ML; Dalton JT; Miller DD Arylisothiocyanato selective androgen receptor modulators (SARMs) for prostate cancer. *Bioorg. Med. Chem.* 2006, 14, 6525–6538. [PubMed: 16828557]
- (12). Bohl CE; Wu Z; Chen J; Mohler ML; Yang J; Hwang DJ; Mustafa S; Miller DD; Bell CE; Dalton JT Effect of B-ring substitution pattern on binding mode of propionamide selective androgen receptor modulators. *Bioorg. Med. Chem. Lett.* 2008, 18, 5567–5570. [PubMed: 18805694]
- (13). Hwang DJ; He Y; Ponnusamy S; Mohler ML; Thiyagarajan T; McEwan IJ; Narayanan R; Miller DD New Generation of Selective Androgen Receptor Degraders: Our Initial Design, Synthesis, and Biological Evaluation of New Compounds with Enzalutamide-Resistant Prostate Cancer Activity. *J. Med. Chem.* 2019, 62, 491–511. [PubMed: 30525603]
- (14). Jones A; Chen J; Hwang DJ; Miller DD; Dalton JT Preclinical characterization of a (S)-N-(4-cyano-3-trifluoromethylphenyl)-3-(3-fluoro, 4-chlorophenoxy)-2-hydroxy-2-methylpropanamide: a selective androgen receptor modulator for hormonal male contraception. *Endocrinology* 2009, 150, 385–395. [PubMed: 18772237]

- (15). Jones A; Hwang DJ; Duke CB 3rd; He Y; Siddam A; Miller DD; Dalton JT Nonsteroidal selective androgen receptor modulators enhance female sexual motivation. *J. Pharm. Exp. Ther.* 2010, 334 (2), 439–448.
- (16). Kim J; Wu D; Hwang DJ; Miller DD; Dalton JT The para substituent of S-3-(phenoxy)-2-hydroxy-2-methyl-N-(4-nitro-3trifluoromethyl-phenyl)-propionamides is a major structural determinant of in vivo disposition and activity of selective androgen receptor modulators. *J. Pharm. Exp. Ther.* 2005, 315, 230–239.
- (17). Jones A; Hwang DJ; Narayanan R; Miller DD; Dalton JT Effects of a novel selective androgen receptor modulator on dexamethasone-induced and hypogonadism-induced muscle atrophy. *Endocrinology* 2010, 151, 3706–3719. [PubMed: 20534726]
- (18). Li W; Hwang DJ; Cremer D; Joo H; Kraka E; Kim J; Ross CR 2nd; Nguyen VQ; Dalton JT; Miller DD. Structure determination of chiral sulfoxide in diastereomeric bicalutamide derivatives. *Chirality* 2009, 21, 578–583. [PubMed: 18726944]
- (19). Mohler ML; Bohl CE; Jones A; Coss CC; Narayanan R; He Y; Hwang DJ; Dalton JT; Miller DD Nonsteroidal selective androgen receptor modulators (SARMs): dissociating the anabolic and androgenic activities of the androgen receptor for therapeutic benefit. *J. Med. Chem.* 2009, 52, 3597–3617. [PubMed: 19432422]
- (20). Dalton JT; Mukherjee A; Zhu Z; Kirkovsky L; Miller DD Discovery of nonsteroidal androgens. *Biochem. Biophys. Res. Commun.* 1998, 244, 1–4. [PubMed: 9514878]
- (21). Ponnusamy S; Coss CC; Thiyagarajan T; Watts K; Hwang DJ; He Y; Selth LA; McEwan IJ; Duke CB; Pagadala J; et al. Novel Selective Agents for the Degradation of Androgen Receptor Variants to Treat Castration-Resistant Prostate Cancer. *Cancer Res.* 2017, 77, 6282–6298. [PubMed: 28978635]
- (22). Ponnusamy S; He Y; Hwang DJ; Thiyagarajan T; Houtman R; Bocharova V; Sumpter BG; Fernandez E; Johnson D; Du Z; et al. Orally Bioavailable Androgen Receptor Degradator, Potential Next-Generation Therapeutic for Enzalutamide-Resistant Prostate Cancer. *Clin. Cancer Res.* 2019, 25, 6764–6780. [PubMed: 31481513]
- (23). He Y; Hwang DJ; Ponnusamy S; Thiyagarajan T; Mohler ML; Narayanan R; Miller DD Pyrazol-1-yl-propanamides as SARD and Pan-Antagonists for the Treatment of Enzalutamide-Resistant Prostate Cancer. *J. Med. Chem.* 2020, 63, 12642–12665. [PubMed: 33095584]
- (24). He Y; Hwang DJ; Ponnusamy S; Thiyagarajan T; Mohler ML; Narayanan R; Miller DD Exploration and Biological Evaluation of Basic Heteromonocyclic Propanamide Derivatives as SARDs for the Treatment of Enzalutamide-Resistant Prostate Cancer. *J. Med. Chem.* 2021, 64, 11045–11062. [PubMed: 34269581]
- (25). Stepan AF; Mascitti V; Beaumont K; Kalgutkar AS Metabolism-guided drug design. *Med. Chem. Commun.* 2013, 4, 631–652.
- (26). Blier P; Bergeron R The use of pindolol to potentiate antidepressant medication. *J. Clin. Psychiatry* 1998, 59 (Suppl 5), 16–23. discussion 24–15
- (27). Esatbeyoglu T; Wagner AE; Schini-Kerth VB; Rimbach G Betanin—a food colorant with biological activity. *Mol. Nutr. Food Res.* 2015, 59, 36–47. [PubMed: 25178819]
- (28). Romero DL; Morge RA; Biles C; Berrios-Pena N; May PD; Palmer JR; Johnson PD; Smith HW; Busso M; et al. Discovery, synthesis, and bioactivity of bis(heteroaryl)piperazines. 1. A novel class of non-nucleoside HIV-1 reverse transcriptase inhibitors. *J. Med. Chem.* 1994, 37, 999–1014. [PubMed: 7512142]
- (29). Sravanthi TV; Manju SL Indoles - A promising scaffold for drug development. *Eur. J. Pharm. Sci.* 2016, 91, 1–10. [PubMed: 27237590]
- (30). Hubbard TD; Murray IA; Perdew GH Indole and Tryptophan Metabolism: Endogenous and Dietary Routes to Ah Receptor Activation. *Drug metab. dispos.: the biological fate of chemicals* 2015, 43, 1522–1535.
- (31). Hedner T; Edgar B; Edvinsson L; Hedner J; Persson B; Pettersson A Yohimbine pharmacokinetics and interaction with the sympathetic nervous system in normal volunteers. *Eur. J. Clin. Pharmacol.* 1992, 43, 651–656. [PubMed: 1493849]
- (32). Boriskin YS; Leneva IA; Pecheur EI; Polyak SJ Arbidol: a broad-spectrum antiviral compound that blocks viral fusion. *Curr. Med. Chem.* 2008, 15 (10), 997–1005. [PubMed: 18393857]

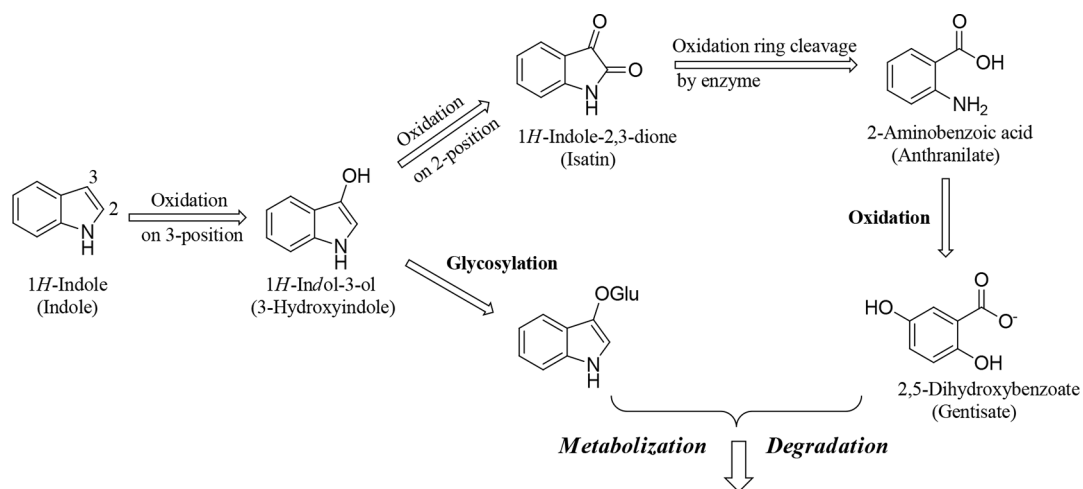
- (33). Claus G; Kutzner HJ Degradation of indole by *Alcaligenes spec.* Syst. Appl. Microbiol. 1983, 4, 169–180. [PubMed: 23194589]
- (34). Lima MB, Glycation J,W; In Encyclopedia of Biological Chemistry, 2nd Ed.; Academic Press, 2013; pp 405–411.
- (35). Banjare SK; Nanda T; Ravikumar PC Cobalt-Catalyzed Regioselective Direct C-4 Alkenylation of 3-Acetylindole with Michael Acceptors Using a Weakly Coordinating Functional Group. Org. Lett. 2019, 21, 8138–8143. [PubMed: 31545620]
- (36). Miyaura N; Yamada K; Suzuki A A new stereospecific cross-coupling by the palladium-catalyzed reaction of 1-alkenylboranes with 1-alkenyl or 1-alkynyl halides. Tetrahedron Lett. 1979, 20, 3437–3440.
- (37). Soubhye J; Prevost M; Van Antwerpen P; Zouaoui Boudjeltia K; Rousseau A; Furtmuller PG; Obinger C; Vanhaeverbeek M; Ducobu J; Neve J; et al. Structure-based design, synthesis, and pharmacological evaluation of 3-(aminoalkyl)-5-fluoroindoles as myeloperoxidase inhibitors. J. Med. Chem. 2010, 53, 8747–8759. [PubMed: 21090682]



**Figure 1.** Known small-molecule AR ligands. These include nonsteroidal and steroidal antagonists (left panel), AR agonists (middle panel) and initial AR antagonists and AR degraders (right panel).

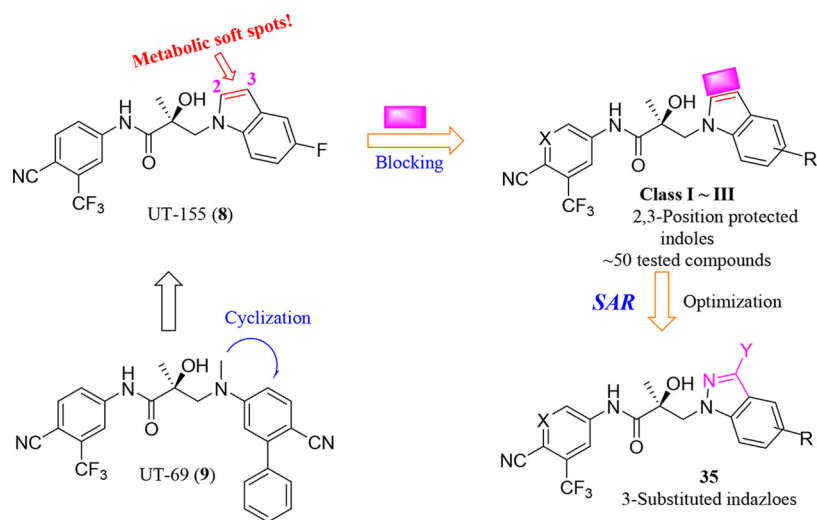


**Figure 2.** Natural bioactive alkaloids (compounds 11, 14–15) and synthesized drugs (compounds 10, 12–13, and 16–18) containing an indole nucleus that is (A) unsubstituted; (B) substituted at the 2-position; (C) substituted at the 3-position; or (D) substituted at both the 2- and 3-positions.

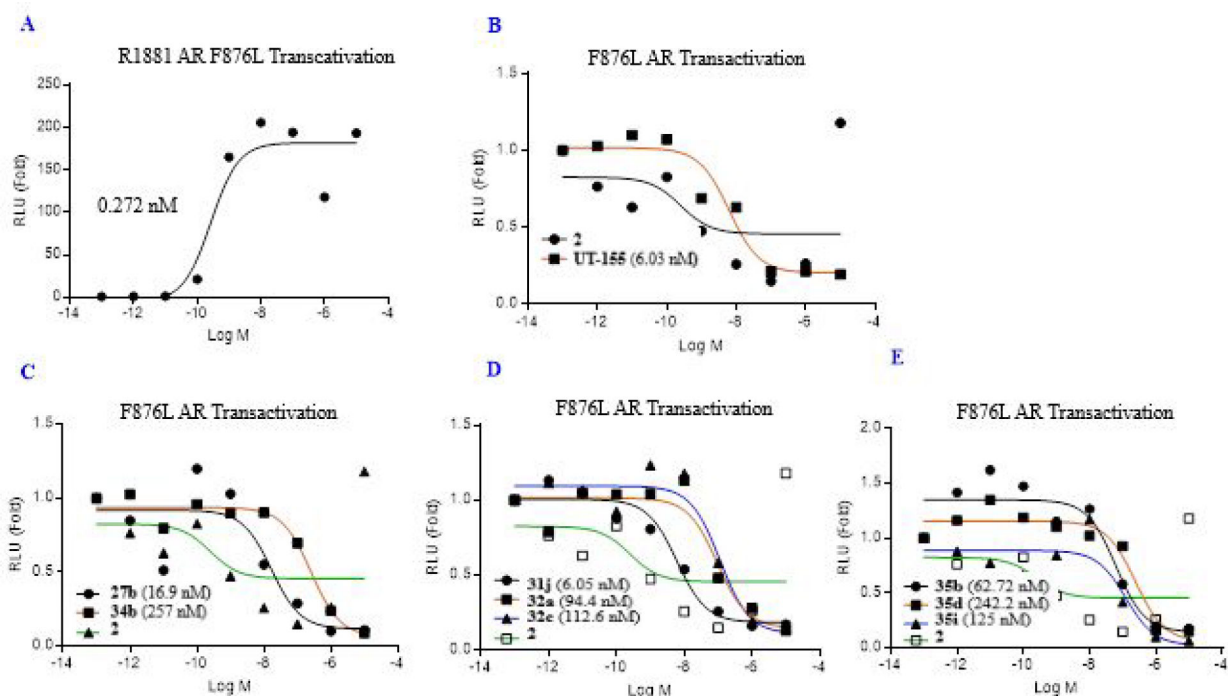


**Figure 3.** Proposed mechanism for *in vivo* and/or *in vitro* metabolic degradation of an indole.<sup>33,34</sup> Oxidation at the 3-position of the indole ring and its subsequent glycosylation results in its degradation. Alternatively, oxidation at the 3-position and subsequently at the 2-position leads to oxidative cleavage of the five-membered pyrrole constituent of the heterobicyclic ring by a cellular enzyme. Further oxidation results in degradation of the ring.



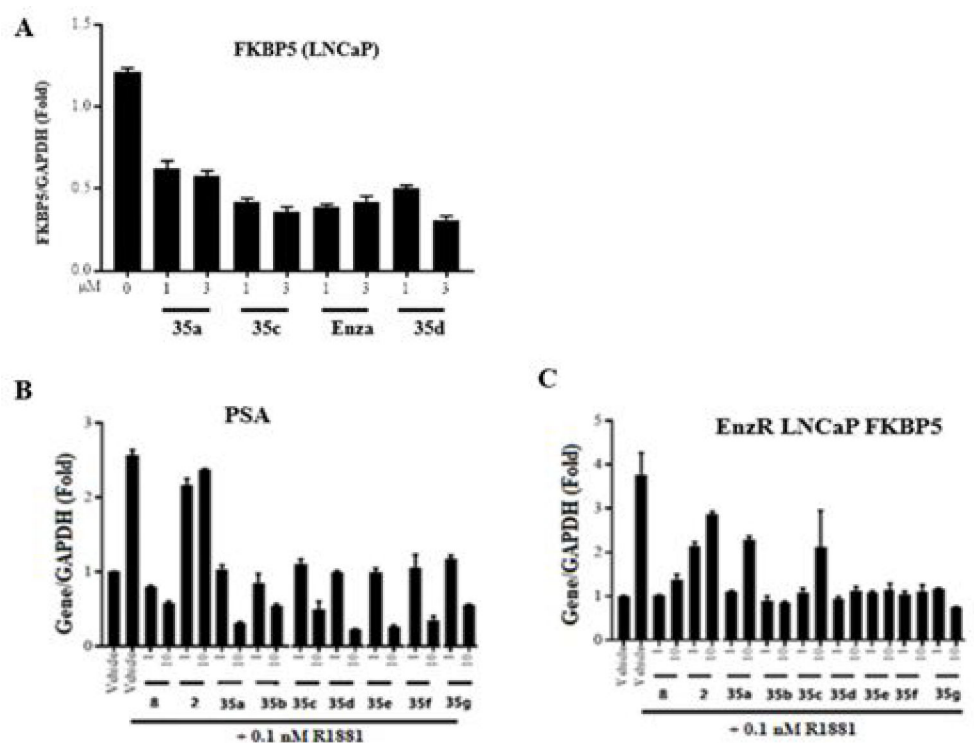


**Figure 4.**  
Design and SAR study for metabolically stable 2,3-substituted indoles.

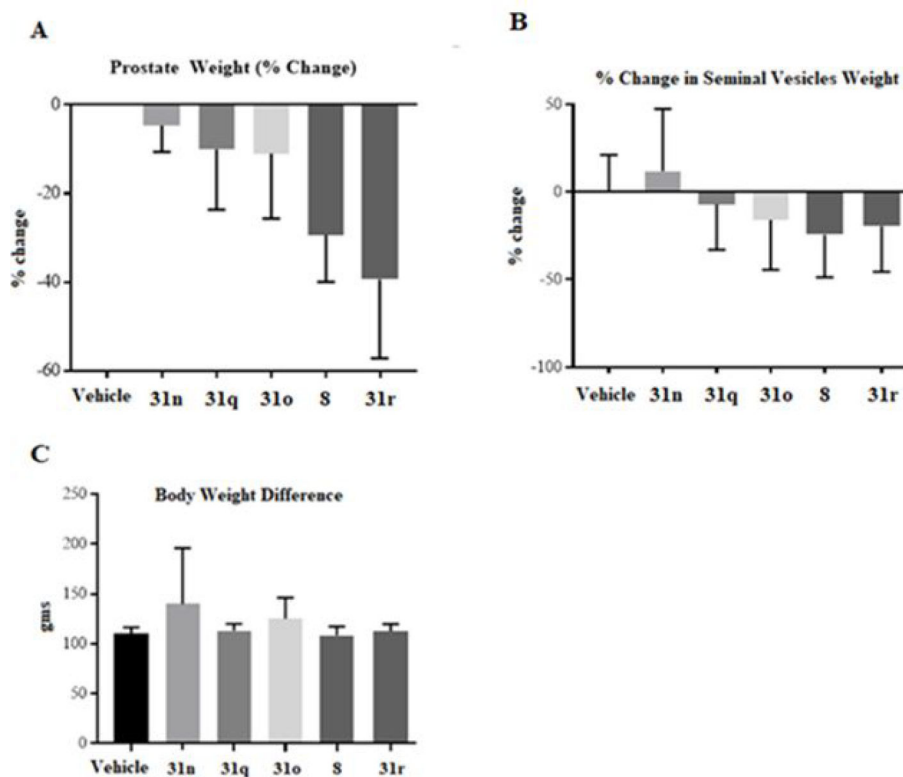


**Figure 5.**

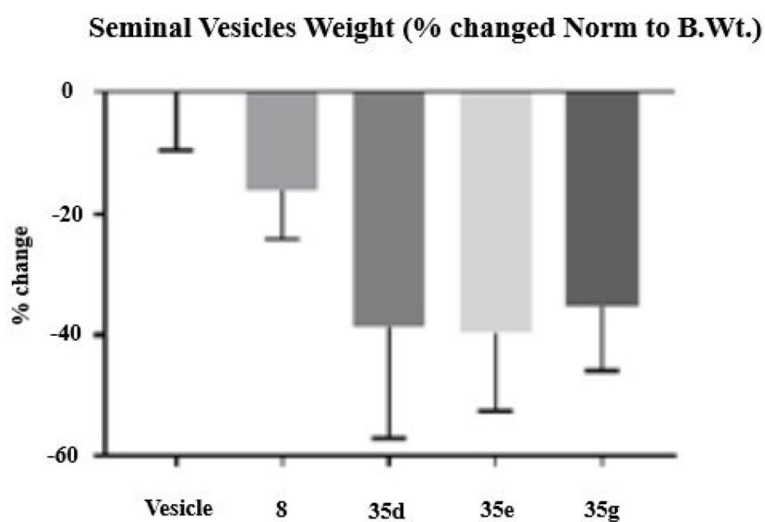
Class I–III antagonism of F876L mutant AR transactivation. (A) R1881. (B) Enzalutamide (2) and UT-155 (8). (C) Class I: carbazole and benzotriazole in B-ring). (D) Class II (benzimidazole and indazole in B-ring). (E) Class III (3-substituted indazoles in B-ring): AR with F876L (phenylalanine 876 mutated to leucine), GRE-LUC, and CMV-renilla LUC transfected in COS cells. Cells treated 24 h after transfection with 0.1 nM R1881 (agonist) and a dose response of antagonists. Luciferase assay performed 48 h after transfection. The effect of each compound conducted in antagonistic mode (in the presence of 0.1 nM R1881). IC<sub>50</sub> values of the Class I–III calculated and provided in the figure.



**Figure 6.** Effect of 35-series compounds on transcription of AR-regulated gene FKBP5 and PSA in prostate cancer LNCaP cells, and FKBP5 in enzalutamide-resistant LNCaP cells. (A-B) LNCaP cells or (C) enzalutamide-resistant LNCaP cells were plated and maintained in RPMI+1%FBS medium for 2 days prior to treatment with AR agonist R1881 (0.1 nM) and the drug indicated in the figure as antagonist (1, 3, or 10  $\mu$ M). After 24h, total RNA was isolated, analyzed by quantitative reverse transcription polymerase chain reaction (RT-qPCR) with the indicated primers and probes. Signals were normalized to those of glyceraldehyde-3-phosphate dehydrogenase (GAPDH). Detection of mRNA encoding (A) AR target gene FKBP5, (B) prostate-specific antigen (PSA), or (C) FKBP5 in enzalutamide-resistant LNCaP cells. Levels of each mRNA were compared to those after treatment with enzalutamide (compound 2) or (B–C) enzalutamide (compound 2) and UT-155 (compound 8). These compounds antagonized the function of AR in both LNCaP cells and LNCaP cell derivatives that are enzalutamide resistant.

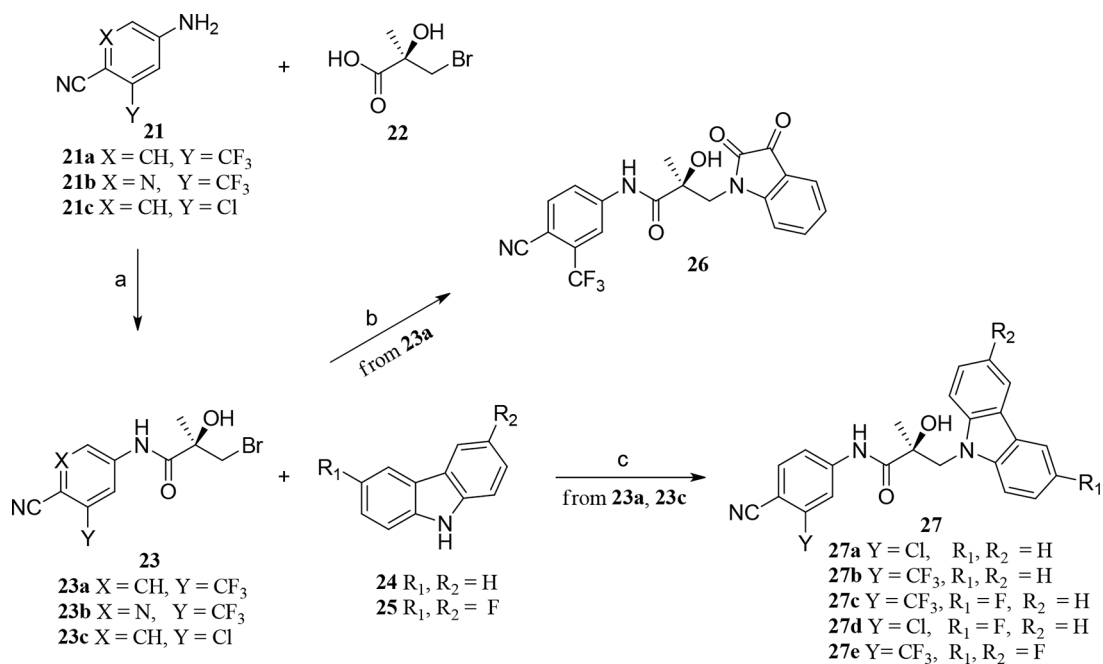


**Figure 7.** *In vivo* antagonism of AR by UT-155 (compound **8**) and series **31** compounds. Growth of androgen-dependent organs in rats using an *in vivo* Hershberger assay.<sup>21–24</sup> Rats were treated orally ( $n = 5/\text{group}$ ) for 14 d with 40 mg/kg/day of a vehicle, either indicated **31** series compounds or compound **8**. Animals were sacrificed, and weights of prostate (A) and seminal vesicles (B) were measured and normalized to body weight. (C) Body Weight Difference.



**Figure 8.**

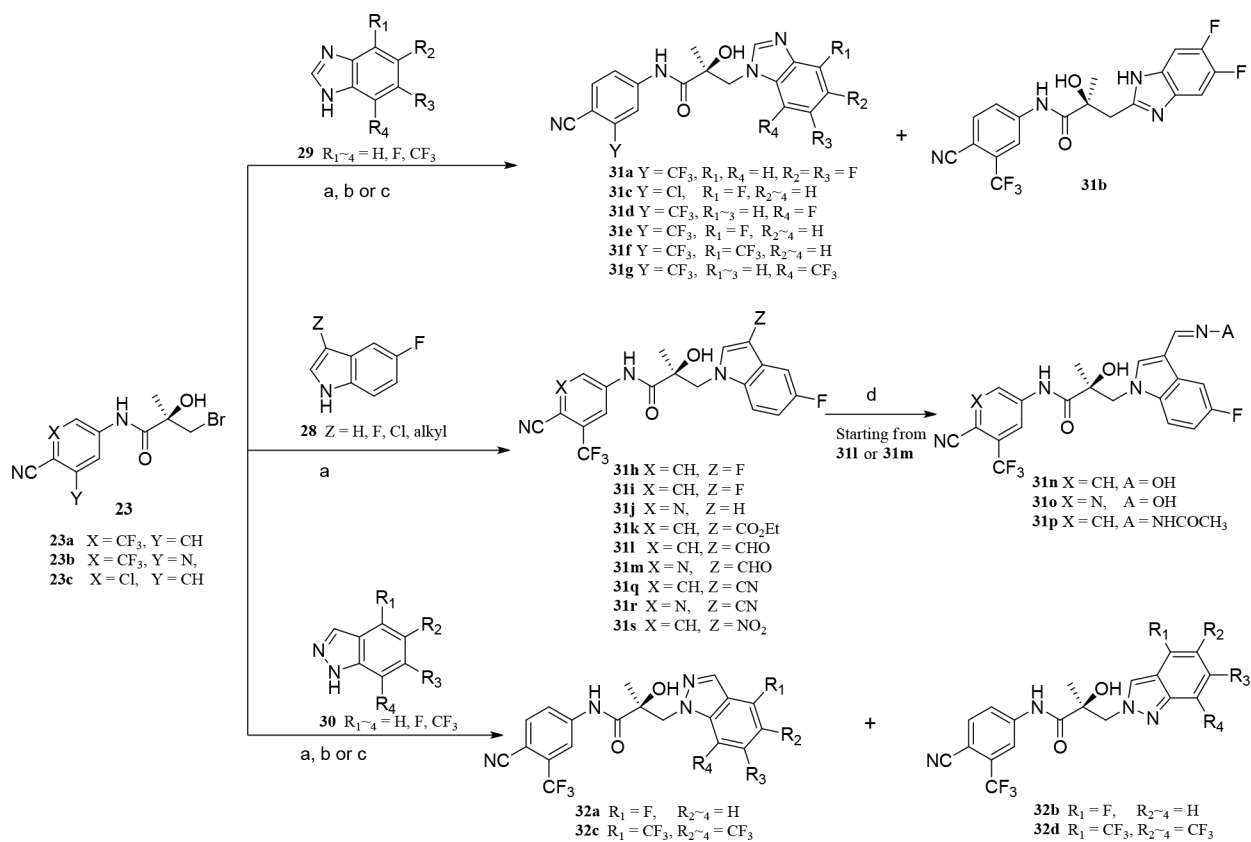
*In vivo* antagonism of **35** series compounds. Male Sprague–Dawley rats (100–120 g) were treated orally with either vehicle or 20 mg/kg of compounds **8**, **35d**, **35e**, or **35g** for 13 days. Animals were sacrificed on the 14th day, and seminal vesicle weights were recorded. The inhibition of androgen-dependent seminal vesicle growth, measured as loss of organ weight by **8**, **35d**, **35e**, and **35g** vs vehicle, was statistically significant ( $p = 0.0031$ ).  $N = 5$ /group.



**Scheme 1. Generic Synthesis of Class I Compounds 27a–e<sup>a</sup>**

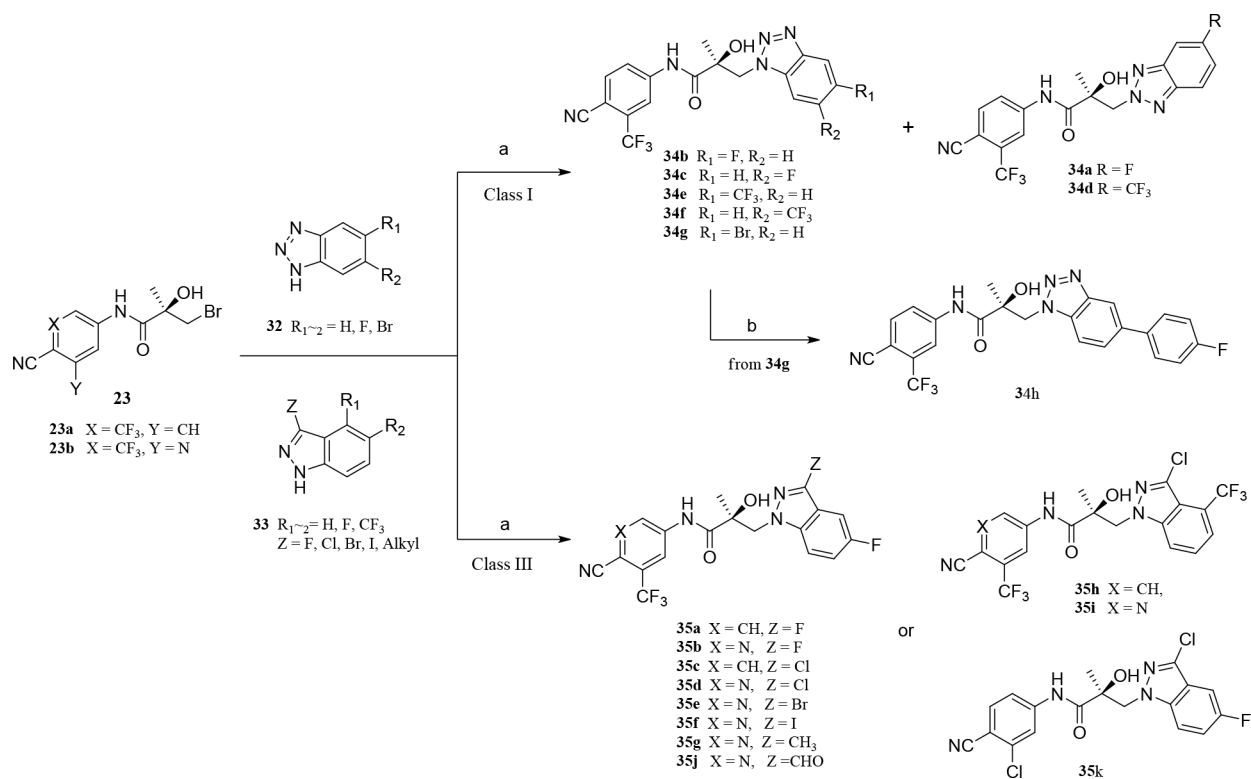
<sup>a</sup>Reagents and conditions: (a) i. SOCl<sub>2</sub>, THF, 0 °C; ii. Et<sub>3</sub>N; (b) isatin, K<sub>2</sub>CO<sub>3</sub>, DMF, room temperature (RT); (c) NaH, THF, 0 °C to RT.





**Scheme 2. Generic Synthesis of Class II (Compounds 31a–s and 32a–d)<sup>a</sup>**

<sup>a</sup>Reagents and conditions: (a) NaH, THF, 0 °C to RT; (b) K<sub>2</sub>CO<sub>3</sub>, DMF, 80 °C; (c) bis(trimethylsilyl)-amide, THF, –78 °C ~ RT; (d) NH<sub>2</sub>OH or NH<sub>2</sub>NHCOCH<sub>3</sub>, pyridine, RT.








**Scheme 3. Generic Synthesis of Class I (34a–h) and III (35a–g) Compounds<sup>a</sup>**

<sup>a</sup>Reagents and conditions: (a) compound **32** or **33**, NaH, THF, 0 °C to RT; (b) Pd(PPh<sub>3</sub>)<sub>3</sub>, Na<sub>2</sub>CO<sub>3</sub>, phenylboronic acid, EtOH/H<sub>2</sub>O, reflux.

Table 1.

## Initial Biological Evaluation of Indole AR Analogues

ID	Structure	Binding ( $K_i$ )/Transactivation ( $IC_{50}$ ) ( $\mu$ M)		SARD Activity (% degradation)		Metabolic Stability in Mouse Liver Microsomes (MLM) <sup>f</sup>	
		$K_i$ (DHT = 1 nM) <sup>a</sup>	$IC_{50}$ <sup>b</sup>	Full Length <sup>c,d</sup> (LNCaP)@1 $\mu$ M	Splice Variant <sup>c</sup> (22RV1)@10 $\mu$ M	$T_{1/2}$ (min)	$CL_{int}$ (mL/min/mg)
8 <sup>13</sup>		0.267	0.085	76	87	12.35	5.614
19a <sup>13</sup>		0.547	0.157	32	69	21.77	3.184
19b		0.332	0.045	68	62	9.29	7.46
20		0.757	0.027	57, 97 <sup>d</sup>	N/A <sup>e</sup>	14.6	4.70
26		>10	>10	0	0	N/A <sup>e</sup>	N/A <sup>e</sup>

<sup>a</sup> AR binding was determined by competitive ligand binding, as described.<sup>13,21,23,24</sup> The recombinant ligand binding domain (LBD) of wildtype AR was incubated with 1 nM [<sup>3</sup>H]-mibolerone and the candidate SARD compound (1 pM – 100  $\mu$ M) or 1 nM DHT; following incubation, the complex was precipitated with hydroxyapatite and washed, and the bound radioactivity was eluted and quantified on a scintillation counter. SigmaPlot software was used to determine the resulting inhibitory constant ( $K_i$ ) for each compound relative to 1 nM DHT.

<sup>b</sup> Inhibition of AR transactivation was determined by transfecting human embryonic kidney HEK-293 cells with full-length wildtype AR, GRE-LUC, and CMV-renilla luciferase as a transfection control. Twenty-four h later, the cells were treated for 24 h with 0.1 nM agonist R1881 or varying doses of the indicated antagonist compounds (1 pM to 10  $\mu$ M in log units). After incubation, the cells were collected, lysed, and analyzed by luciferase assay, as described.<sup>13,21</sup>

<sup>c</sup> SARD activity was determined as a function of AR protein levels in cultured cells, as described.<sup>13,21,22</sup> Cells used were of the androgen-sensitive human prostate adenocarcinoma cell line LNCaP that expresses full-length (FL) AR or the xenograft-derived human prostate carcinoma epithelial cell line 22RV1 that expresses a c-terminally truncated splice variant (SV) of AR (AR-V7). Cells were treated

for 24 h with the indicated doses of the candidate antagonist compounds in the presence of 0.1 nM agonist R1881. Cells were harvested, lysed, and FL or SV AR was detected by immunoblot with AR-N20 antibodies directed against the AR N-terminal domain (NTD). Blots were stripped and reprobed with antibodies specific for the cellular protein actin as an internal control. FL and SV AR species were quantified and normalized to actin signals.

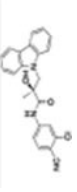
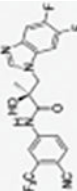
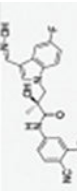
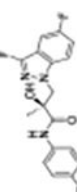
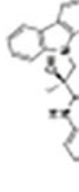
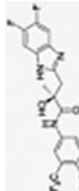
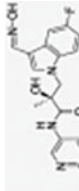
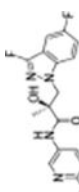
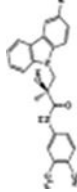
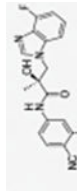

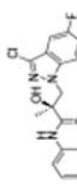
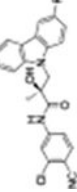
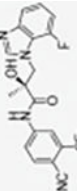
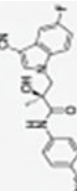
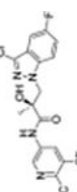
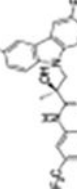
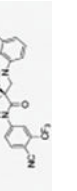
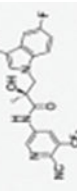
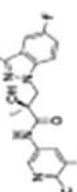
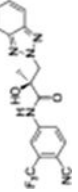
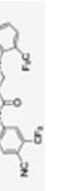
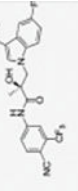

<sup>d</sup> SARD activity of compound **20** against FL AR was evaluated in LNCaP cells at 10  $\mu$ M concentration.

<sup>e</sup> SARD activity of compound **20** against SV AR in 22RV1 cells was not available (N/A).

<sup>f</sup> The metabolic stability (half-life, hepatic clearance) of each compound was determined by incubation for varying time periods with mouse liver microsomes (MLM) and cofactors for phase I and phase II metabolism, as described in the Experimental section in Supporting Information.  $T_{1/2}$  (h) after oral administration in humans as previously reported.<sup>1,3</sup> CL (mL/h/kg) after oral administration in humans as previously reported.<sup>2,3,24</sup>

Table 2.

Summary of Structures of Designed Molecules (Class I, II, and III)

ID	Structure	ID	Structure	ID	Structure	ID	Structure
27a		31a*		31n		35a	
27b		31b*		31o		35b	
27c		31c		31p		35c	
27d		31d*		31q		35d	
27e		31e*		31r		35e	
34a		31f*		31s		35f	

ID	Structure	ID	Structure	ID	Structure	ID	Structure
<b>34b</b>		<b>31g*</b>		<b>32a<sup>§</sup></b>		<b>35g</b>	
<b>34c</b>		<b>31h</b>		<b>32b<sup>§</sup></b>		<b>35h</b>	
<b>34d</b>		<b>31i</b>		<b>32c<sup>§</sup></b>		<b>35i</b>	
<b>34e</b>		<b>31j</b>		<b>32d<sup>§</sup></b>		<b>35j</b>	
<b>34f</b>		<b>31k</b>				<b>35k</b>	
<b>34g</b>		<b>31l</b>					
<b>34h</b>		<b>31m</b>					

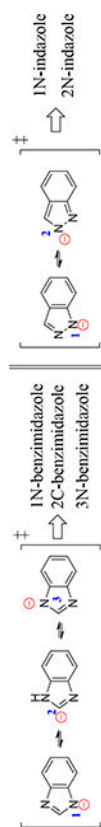
\* The compounds contained regioisomers of benzimidazoles in indole B-rings (**31a** and **31b**, **31d** and **31e**, **31f** and **31g**, i.e., 1N-, 2C-, or 3N-substituted).

<sup>§</sup>Regioisomers of indazoles in indole B-rings (**32a** and **32b**, **32c** and **32d**, i.e., 1N- or 2N-substituted).



Table 3.

Regiospecific Isomers of Benzimidazole and Indazole in B-Ring Derivatives



ID	Structure	Represented name	ID	Structure	Represented name
31a		1N-benzimidazole	32a		1N-indazole
31b		2C-benzimidazole	32b		2N-indazole
31g		1N-benzimidazole	32c		1N-indazole
31f		3N-benzimidazole	32d		2N-indazole

**Table 4.***In Vitro* Pharmacological Activity of Class I Derivatives (Compounds 27a–e and 34a–h)<sup>a</sup>

Class I (ID)	Binding (K <sub>i</sub> )/Transactivation (IC <sub>50</sub> ) (μM)		SARD Activity (% degradation)	
	K <sub>i</sub> (DHT=1nM) <sup>b</sup>	IC <sub>50</sub> <sup>b</sup>	Full Length <sup>b</sup> (LNCaP) @1 μM	Splice Variant <sup>b</sup> (22RV1) @10 μM
<b>8</b>	0.267	0.085	76	87
<b>27a</b>	0.091	1.079	19, 87 <sup>e</sup>	87
<b>27b</b>	0.729	0.871	48	60
<b>27c</b>	0.194	0.991	20	29
<b>27d</b>	0.249	1.243	38	0 <sup>g</sup>
<b>27e</b>	0.810	1.025	51	<sub>f</sub>
<b>34a</b>	3.615	0.277	70	0 <sup>g</sup>
<b>Class I 34b</b>	>100	0.687	60	0 <sup>g</sup>
<b>34c</b>	1.476	0.560	40	0 <sup>g</sup>
<b>34d</b>	>100	>100	<sub>f</sub>	<sub>f</sub>
<b>34e</b>	>100	N/A <sup>f</sup>	<sub>f</sub>	<sub>f</sub>
<b>34f</b>	>100	<sub>g</sub>	<sub>f</sub>	<sub>f</sub>
<b>34g</b>	>100	2.594	<sub>f</sub>	<sub>f</sub>
<b>34h</b>	>100	>100	<sub>f</sub>	<sub>f</sub>
<b>1</b> [ <i>R</i> -Bicalutamide]	0.509	0.248	0 <sup>g</sup>	0 <sup>g</sup>
<b>2</b> [Enzalutamide]	3.641	0.216	0 <sup>g</sup>	0 <sup>g</sup>
<b>4</b> [Darolutamide]	4.231	0.048	<sub>f</sub>	<sub>f</sub>
<b>6</b> [Enobosarm] <sup>c</sup>	0.0038	0.0038 <sup>c</sup>	Agonist <sup>d</sup>	Agonist <sup>d</sup>

<sup>a</sup>Class I and II derivatives were in which the B-ring was substituted quinoline, carbazole, or benzotriazole were found to be selective androgen receptor degraders (SARDs).

<sup>b</sup>AR binding, transactivation, and degradation assays were performed.

<sup>c</sup>*In vitro* transcriptional activation was run in agonist mode for which the EC<sub>50</sub> value was previously reported.<sup>13</sup>

<sup>d</sup>The full agonist Enobosarm (compound **6**) increases AR protein expression.

<sup>e</sup>*In vitro* transcriptional activation was run in antagonist mode for which the IC<sub>50</sub> value was previously reported.<sup>13</sup> Tested at 10 μM concentration.

<sup>f</sup>Not available (N/A).

<sup>g</sup>No effect.

**Table 5.**

*In Vitro* Pharmacological Activity of Class II and III B-Ring Derivatives (Compounds 31a–s, 32a–f, and 35a–k)<sup>a</sup>

Class	Binding (K <sub>i</sub> )	Transactivation (IC <sub>50</sub> ) (μM)	SARD Activity (% degradation)	
(ID)	K <sub>i</sub> (DHT=1nM) <sup>b</sup>	IC <sub>50</sub> <sup>b</sup> IC50	Full Length <sup>b</sup> (LNCaP) @1 μM	Splice Variant <sup>b</sup> (22RV1) @10 μM
<b>8</b>	0.267	0.085	76	87
<b>31a</b>	0.724	0.999	7, 68 <sup>c</sup>	_d
<b>31b</b>	1.399	0.721	51	0
<b>31c</b>	0.883	1.662	0	75
<b>31d</b>	0.913	0.371	0	0
<b>31e</b>	1.589	1.024	0	78
<b>31f</b>	0.493	>100	50	0
<b>31g</b>	0.474	3.616	64	0
<b>31h</b>	0.318	0.274	72	84
<b>31i</b>	0.755	0.367	60	80
<b>31j</b>	0.757	0.021	57, 97 <sup>c</sup>	_d
<b>Class II</b>	<b>31m</b> >100	0.746	0, 83 <sup>c</sup>	_d
	<b>31n</b> >100	0.583	78	56
	<b>31o</b> >100	0.134	44, -2 <sup>c</sup>	15
	<b>31p</b> >100	3.434	_d	_d
	<b>31q</b> >100	0.160	66, 90 <sup>c</sup>	45
	<b>31r</b> 0.644	0.488	112, -69 <sup>c</sup>	25
	<b>31s</b> 0.424	0.063	_d	_d
	<b>32a</b> 0.137	0.173	92	34
	<b>32b</b> 0.172	>100	0	0
	<b>32c</b> 1.006	0.373	84	100
	<b>32d</b> 12.325	0.209	0	0
	<b>35a</b> 0.605	0.102	37, 81 <sup>c</sup>	53
	<b>35b</b> >100	0.0267	66, 78 <sup>c</sup>	_d
	<b>35c</b> 1.343	0.165	34, 46 <sup>c</sup>	_d
	<b>35d</b> 3.006	0.183	36, 36 <sup>c</sup>	_d
	<b>35e</b> 26.302	0.162	-15, 6.3 <sup>c</sup>	_d
<b>Class III</b>	<b>35f</b> 3.268	0.237	21, 101 <sup>c</sup>	_d
	<b>35g</b> >100	0.0891	22, 37 <sup>c</sup>	_d
	<b>35h</b> >100	0.0485	11, 20 <sup>c</sup>	_d
	<b>35i</b> >100	0.02097	-4	_d
	<b>35j</b> 0.796	0.1156	37	_d
	<b>35k</b> >100	0.796	20, 22 <sup>c</sup>	_d

<sup>a</sup>Class II and III derivatives with B-ring 3-position substituted indole, benzimidazole or indazole groups are selective androgen receptor degraders (SARDs).

<sup>b</sup>AR binding, transactivation, and degradation assays were performed, and values were reported in Table 1.

<sup>c</sup>Assessed at 10  $\mu\text{M}$  concentration.

<sup>d</sup>N/A, not available.

Author Manuscript

Author Manuscript

Author Manuscript

Author Manuscript

**Table 6.** *In Vitro* Metabolic Stability Of Class I, II, and III in Mouse Liver Microsomes (MLM)

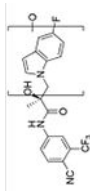
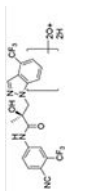
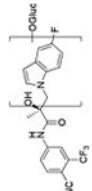
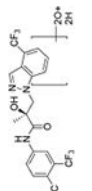
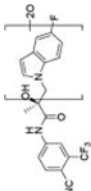
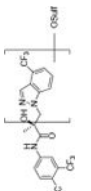
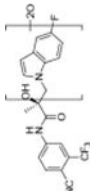
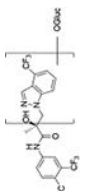
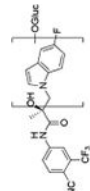
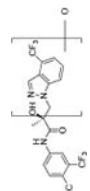
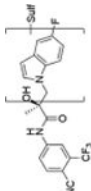
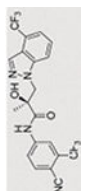
ID	DMPK (MLM) <sup>d</sup>		ID	DMPK (MLM) <sup>d</sup>		
	T <sub>1/2</sub> (min)	CL <sub>int</sub> (mL/min/mg)		T <sub>1/2</sub> (min)	CL <sub>int</sub> (mL/min/mg)	
Class I	27b	41.77	1.66	35b	45.00	
	27c	39.94	1.735	35c	23.66	
	31h	7.70	8.90	35d	49.46	
Class II	31i	23.44	2.96	35g	22.60	
	31j	14.60	4.70	35h	105.00	
	31l	55.00	1.30	35i	120.60	
	31o	50.15	1.40			
31q	12.63	5.5				
32a	13.29	5.2	8 <sup>22</sup>	Antagonist	12.35	5.614
32c	53.71	1.29	1	Antagonist	10.04 <sup>b</sup>	86.3 <sup>16</sup>
32d	35.46	1.96	6	Agonist	360.00	1.4 <sup>16</sup>

<sup>a</sup>Compounds were incubated with MLM and cofactors for phases I and II, as described in the Experimental Section.

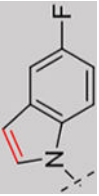
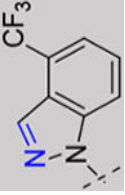
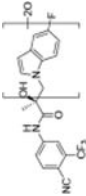
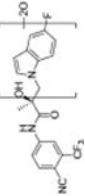
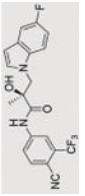
<sup>b</sup>T<sub>1/2</sub> (h) as previously reported,<sup>19,20</sup>

Table 7.

Comparison of Deprotonated Molecular Ions for Compounds 8 and 32c and Identified Metabolites

Panel A		Compound 8		Panel B		Compound 32c	
Metabolite Designation	Retention time (min)	[M - H] <sup>-</sup>	Proposed Metabolite Identification	Metabolite Designation	Retention time (min)	[M - H] <sup>-</sup>	Proposed Metabolite Identification
M1	17.73 <sup>a</sup>	420		M1(3)	18.20 <sup>d</sup>	489	
M2	17.79 <sup>a</sup>	596		M2	18.37 <sup>d</sup>	489	
M3	17.97 <sup>b</sup>	436		M3(2)	18.68 <sup>d</sup>	551	
M4(2)	18.13 <sup>a</sup>	436		M4(1)	19.17 <sup>d</sup>	647	
M5(3)	18.29 <sup>a</sup>	596		M5	20.25 <sup>d</sup>	471	
M6	18.99 <sup>a</sup>	500		32c	20.88 <sup>d</sup>	455	



Panel A		Compound 8		Panel B		Compound 32c	
Metabolite Designation	Retention time (min)	[M - H] <sup>-</sup>	Proposed Metabolite Identification	Metabolite Designation	Retention time (min)	[M - H] <sup>-</sup>	Proposed Metabolite Identification
M7	19.10 <sup>a</sup>	420					
M8(1)	19.62 <sup>a</sup>	580					
M9	19.64 <sup>a</sup>	420					
UT-155 (8)	20.52 <sup>a</sup>	404					

<sup>a</sup>Retention time from analysis of human AR.

<sup>b</sup>Retention time from analysis of mouse AR.

<sup>c</sup>Biological Experiments are described in Supplemental Section 3-1.1. This study was conducted by Covance Laboratories Inc., 3301 Kinsman Boulevard, Madison, WI, in accordance with the protocol and Covance standard operating procedures (SOPs).

**Table 8.** Relative Abundance of Identified Metabolites for UT-155 (Compound 8) in Each Species

M # <sup>a</sup>	[M – H] <sup>-</sup>	Mass Shift	Peak areas (× 10 <sup>3</sup> )				
			Human	Rat	Dog	Monkey	Mouse
M1	420.0971	15.9949	169	152 *** <sup>c</sup>	NA <sup>b</sup>	NA <sup>b</sup>	NA <sup>b</sup>
M2	596.1282	192.0270	569	267 *** <sup>c</sup>	225 *** <sup>c</sup>	NA <sup>b</sup>	111 *** <sup>c</sup>
M3	436.0920	31.9898	0.00	NA <sup>b</sup>	NA <sup>b</sup>	NA <sup>b</sup>	30.4 *** <sup>c</sup>
M4	436.0920	31.9898	1108 *** <sup>c</sup>	18.6	67.3 *** <sup>c</sup>	142 *** <sup>c</sup>	8.15
M5	596.1292	192.0270	729 *** <sup>c</sup>	46.0	8.20	185 *** <sup>c</sup>	12.3
M6	500.0539	95.9517	283	333 *** <sup>c</sup>	NA <sup>b</sup>	NA <sup>b</sup>	NA <sup>b</sup>
M7	420.0971	15.9949	603	NA <sup>b</sup>	479 *** <sup>c</sup>	NA <sup>b</sup>	129 *** <sup>c</sup>
M8	580.1343	176.0321	1913 *** <sup>c</sup>	0.00	0.00	13.9	0.00
M9	420.0971	15.9949	38.5	NA <sup>b</sup>	NA <sup>b</sup>	23.7 *** <sup>c</sup>	NA <sup>b</sup>

<sup>a</sup>M #, Metabolite number.

<sup>b</sup>NA, not assessed.

<sup>c</sup>\*, Most abundant metabolite in species; \*\*, second most abundant; and \*\*\*, third most abundant.

**Table 9.** Relative Abundance of Identified Metabolites for Compound 32c in Each Species

M # <sup>a</sup>	[M - H] <sup>-</sup>	Mass Shift	Peak areas ( $\times 10^3$ )				
			Human	Rat	Dog	Monkey	Mouse
M1	489.1054	34.9955	286 <sup>***c</sup>	74.8 <sup>***c</sup>	20.7 <sup>***c</sup>	111	49.8
M2	489.1054	34.9955	254	NA <sup>b</sup>	NA	150 <sup>***c</sup>	NA
M3	551.0460	192.0270	1122 <sup>**c</sup>	583 <sup>**c</sup>	36.0 <sup>**c</sup>	839 <sup>**c</sup>	52.7 <sup>***c</sup>
M4	647.1287	192.0270	6147 <sup>*c</sup>	3460 <sup>*c</sup>	208 <sup>*c</sup>	7131 <sup>*c</sup>	1206 <sup>*c</sup>
M5	471.0892	15.9949	28.5	NA	19.4	NA	1170 <sup>**c</sup>

<sup>a</sup>M #, Metabolite number.

<sup>b</sup>NA, not assessed.

<sup>c</sup>\*, Most abundant metabolite in species; \*\*, second most abundant; and \*\*\*, third most abundant.

Summary of the SAR Study to Compare the Pharmaceutical Properties of Indole UT-155 (Compound 8) Substituted with Class I—III Blocking Groups at the 2- and/or 3-Positions of the B-Ring

**Table 10.**

	<b>B</b>	<b>X</b>	<b>Y</b>	<b>AR LBD Binding (K<sub>i</sub>)</b>	<b>DMPK (half-life; T<sub>1/2</sub>)</b>	<b>EnzR antiandrogenic effect (IC<sub>50</sub>)</b>
Class I	27 CH	carbazole		↓	↑↑	Equal or less
	34 CH	N	N	↓	↑↑	Equal or less
Class II	31 CH or N	CH	N- or C-substituted	Equal or less	↑	Equal or less
	32 CH	N	CH	Equal or less	↑↑	↑
Class III	35 CH or N	N	C-substituted	Equal or less	↑↑↑	↑↑

Class I, II, III

8